Theses and dissertations

1-1-2011

# Optimization of optical signal-to noise ratio by α profile multimode fibre in wireless over fibre link

Muhammad Imran Khan
*Ryerson University*

Follow this and additional works at: http://digitalcommons.ryerson.ca/dissertations

Part of the Electrical and Computer Engineering Commons

# OPTIMIZATION OF OPTICAL SIGNAL-TO-NOISE RATIO BY $\alpha$ PROFILE MULTIMODE FIBRE IN WIRELESS OVER FIBRE LINK

by

Muhammad Imran Khan
Bachelor of Engineering, N.E.D. University, Pakistan, 1994
Master's of Engineering, Dalhousie University, Canada, 2005

A thesis
presented to Ryerson University
in partial fulfillment of the
requirement for the degree of
Master of Applied Science
in the Program of
Electrical and Computer Engeering

Toronto, Ontario, Canada, 2011

## Author's Declaration

I hereby declare that I am the sole author of this thesis.
I authorize Ryerson University to lend this thesis to other institutions or individuals for the
purpose of scholarly research.
 Signature

I further authorize Ryerson University to reproduce this thesis by photocopying or by other
means, in total or in part, at the request of other institutions or individuals for the purpose
of scholarly research.
 Signature

# Instructions on Borrowers

Ryerson University requires the signatures of all persons using or photocopying this thesis. Please sign below, and give address and date.

# Abstract

Optimization of optical signal-to-noise ratio by $\alpha$ profile multimode fibre in wireless over
Fibre link
Master of Applied Science 2011
Muhammad Imran Khan
Electrical and Computer Engineering
Ryerson University

The demand of bandwidth in mobile communication is growing exponentially day-by-day, as the numbers of users have been increasing drastically over the span of last five years. Fibre optics has attracted much attention due to its promising performance and operational cost reduction. In this thesis, the feasibility of using multimode fibre as an inexpensive cell feed in indoor system is investigated. The proposed architecture is analyzed using signal to noise ratio versus GI multimode fibre profile parameter $\alpha$, cumulative signal to noise ratio, and multipath fading in indoor environment. The objectives of this thesis are: (i) designing COFDM based radio-over-fibre communication system, (ii) analyzing the downlink and uplink performance considering impairments in the fibre and wireless channels and investigating the effect of core refractive index profile ($\alpha$) on graded index RoF link, (iii) investigating the effect of COFDM cyclic prefix to the graded index multimode fibre dispersion. The performance is evaluated through theoretical analysis and simulations using Matlab. The downlink and uplink analysis are performed considering all the impairments from the air interface and the RoF link. Thereafter, numerical results are generated for the downlink and uplink to illustrate the performance of the COFDM-RoF architecture.

# Acknowledgments

All eulogy belong to ALLAH, the merciful, the compassionate, the omniscient who has patronized us with His conferred benevolence in all fields of life, including this thesis.

I would like to express my deeply felt gratitude to Professor Dr. Kaamran Raahemifar, my supervisor, who provided generous advice and subject area expertise throughout this entire process. I am also especially thankful for his continued support, understanding, and encouragement throughout my education at Ryerson University.

Special thanks are due to my friends at Ryerson Communication Lab and Microelectronic Lab, especially Dr. Xijia Gu for brilliant perspectives on issues relating to fiber optic communications during the thesis process.

I wish to thank my parents, for their daily prayers, giving me the motivation and strength, and encouraging me to accomplish and achieve my goals. I dedicate this thesis to them with great affection and respect.

Finally, I would like to thank my family for their unceasing love, understanding, and encouragement throughout my life. Last but not least, my deepest, warmest thank belongs to Dr. Michael Cada at Dalhousie University, Halifax, for her immeasurable support and encouragement throughout my graduate studies.

# Contents

# List of Tables

# List of Figures

# List of Symbols

| Greek Symbol | Description |
|---|---|
| $\gamma$ | Path loss exponent |
| $\delta$ | Duration of propagation |
| $\sigma$ | Standard deviation of channel loss |
| $\theta_c$ | Critical angle |
| $\theta_a$ | Angle from the normal light |
| $\theta_b$ | Angle from the refractive light |
| $\theta_{air}$ | Maximum angle in air |
| $\alpha$ | Core refractive index profile |
| $\Delta$ | Function of refractive indexes of core and cladding |
| $\lambda$ | Wavelength of a transmitted signal |
| $\mu$ | Cumulative RMS optical modulation index |
| $\tau$ | Time delay of a signal |
| $\tau_{wlan}$ | Time delay of a WLAN signal |
| $\tau_i$ | Time delay of individual signal |
| $\phi_\beta$ | Phase shift of a WLAN signal |
| $\Re$ | Responsivity of a photodetector |
| $\sigma_{sh}^2$ | Mean square value of shot noise |
| $\sigma_{RIN}^2$ | Mean square value of RIN noise |
| $\sigma_{th}^2$ | Mean square value of thermal noise |
| $\omega_\alpha$ | Carrier frequency of Laser |
| $\omega_c$ | Radian carrier frequency |

| English Symbol | Description |
| --- | --- |
| $S_{wlan}$ | WLAN signal |
| $a$ | Signal amplitude |
| $B$ | Bandwidth of a signal |
| $N$ | Number of data samples |
| $N_g$ | Cyclic prefix samples |
| $A_i$ | Optical signal power of *ith* symbol |
| $C_{Laser}(t)$ | Laser output signal |
| $B_{wlan}$ | Bandwidth of the WLAN system |
| $c(t)$ | Coded waveform for the WLAN system |
| $h_{MMF}(t)$ | Impulse response of multimode fiber |
| $n_{opt}(t)$ | Optical noise |
| $F_{loss,dB}$ | Total fiber loss in dB |
| $F_{e/o}$ | Loss due to electrical to optical conversion |
| $F_{o/e}$ | Loss due to optical to electrical conversion |
| $F_{misc}$ | Losses due to connectors, splitters, and splices |
| $d(t)$ | Data sequence of the WLAN signal |
| $F$ | Noise figure of an amplifier |
| $f$ | Frequency in Hertz |
| $G_m$ | Modulation gain of a laser |
| $G_{opt}$ | Optical post amplifier gain |
| $G_{up,wlan}$ | Gain of an amplifier for the WLAN system in the uplink |
| $I_p$ | Average photocurrent |
| $i_D(t)$ | Total detected current |
| $I_D(t)$ | Mean DC current |
| $i_d(t)$ | Mean AC current |
| $h(t)$ | Impulse response |
| $K$ | Absolute temperature |
| $K_B$ | Boltzmann's constant |
| $L$ | Number of resolvable signal paths |
| $L_{op}$ | Total RF power loss in the ROF link |

| | |
|---|---|
| $L_{wl}$ | RF power loss in the air interface |
| $l_c$ | Optical power loss of a connector |
| $m$ | Optical modulation index |
| $m_{wlan}$ | Optical modulation index of a WLAN signal |
| $n_c$ | Number of optical connectors |
| $n_{op,wlan}$ | Optical noise in the WLAN band |
| $n_{up,air}$ | Noise of the WLAN systems in the air interface (uplink) |
| $n_{up,wl}$ | Noise process of the air interface in the uplink |
| $n_{up,wlan}$ | Noise process of the air interface in the WLAN band (uplink) |
| $n_{wl}(t)$ | Wireless channel noise |
| $n(t)$ | Total noise |
| $P_o$ | Mean optical power detected at the photodetector |
| $P_r$ | Received signal power |
| $P(t)$ | Transmitted signal power |
| $q$ | Electron charge |
| $T_o$ | Absolute temperature |
| $R_{90}$ | 90% confidence coverage radius |
| $R_L$ | Receiver resistance |
| $RIN$ | Parameter of the relative intensity noise |
| $r$ | Distance between a MS and the base station |
| $S$ | Shadowing effect parameter |
| $OSNR_{wlan}$ | OSNR of a downlink WLAN signal |
| $OSNR_{up,wlan}$ | Cumulative OSNR of an uplink WLAN signal |
| $SNR_{air,wlan}$ | SNR of a downlink WLAN signal through the air interface |
| $SNRc$ | Cumulative SNR |
| $t$ | Continuous time |
| $Z_{in}$ | Impedance of a laser |
| $Z_{out}$ | Impedance of an optical receiver |

# List of Abbreviations

| Abbreviations | Description |
| --- | --- |
| 3G | Third-generation |
| 4G | Fourth-generation |
| BPSK | Binary phase shift keying |
| GI | Graded index |
| MMF | Multimode fiber |
| GIMMF | Graded index multimode fiber |
| DC | Direct current |
| COFDM | Coded Frequency Division Multiplexing |
| ISI | Inter symbol interference |
| ICI | Intercarrier interference |
| LAN | Local area network |
| LOS | Line of sight |
| Gbps | Giga bits per second |
| Mbps | Mega bits per second |
| MS | Mobile station |
| PDF | Probability distribution function |
| PSD | Power spectrum density |
| QAM | Quadrature amplitude modulation |
| QPSK | Quadrature phase shift keying |
| SQAM | Staggered quadrature amplitude modulation |
| DFT | Discrete Fourier Transform |
| IFFT | Inverse Fast Fourier Transform |
| FFT | Fast Fourier Transform |
| BER | Bit error ratio |
| RAP | Radio access point |
| RF | Radio Frequency |
| RIN | Relative intensity noise |

| | |
|---|---|
| RMS | Root means square |
| RoF | Radio over fiber |
| OSNR | Optical signal to noise ratio |
| SNR | Signal to noise ratio |
| SNRc | Cumulative signal to noise ratio |
| WLAN | Wireless local area network |
| AWGN | Additive white Gaussian noise |
| BS | Base station |
| CS | Control station |
| NA | Numerical aperture |
| CP | Cyclic prefix |

# Chapter 1

# Introduction

*Communication is the most natural and social of human functions. Communication is the process that distributed information, knowledge, and wisdom among people, the mortar that holds together societies as communities [1].*

Radio over fibre (RoF) refers to a technique where radio frequency (RF) signals are transmitted over optical fibre to provide wireless communication services. Although transmitting RF signals over fibre has many applications such as in cable TV networks and Satellite base stations, the term RoF mostly used in connection with the fibre-wireless (Fi-Wi) communication systems.

There are number of reasons why radio signals need to be transmitted over fibre. Most Fi-Wi systems until now, target providing wireless access to special areas like tunnels, mines and subway stations where outdoor macro base stations do not provide coverage. Furthermore, crowded places like campus premises, supermarkets, airport concourses, and downtown core areas can be cost-effectively served by Fi-Wi networks.

Recently the power of RoF solution was realized during Sydney olympics 2000. RoF technology was used to rapidly set-up microcellular networks for the olympics with more than 500 in-building and outdoor pico-cells. Three GSM operators shared this infrastructure and multi-standard radio (900/1800 MHz GSM) was supported. Each remote antenna units provided $0.8 \times 1.8$ km coverage. Dynamic allocation of network capacity was enabled and more than 500,000 wireless calls were made on the opening day using the RoF infrastructure.

1

The RoF technology is now moving from providing coverage to specialized area into the mainstream as a viable broadband wireless access scheme. There are number of reasons for this emerging prominent role of RoF.

## 1.0.1 RoF to Boost Frequency Reuse

Demand for wireless capacity is rapidly increasing. Surveys have shown that a new wireless subscriber signs up every 2.5 seconds. In Japan this number goes from approximately 60 million in year 2000 to more than 100 million in year 2010, measuring 98.7% penetration by 2010 [2]. The number of cellular and personal communications system (PCS) users in the US has surpassed 100 million. The trend is similar worldwide.

To address the increasing demand, more and more base stations are deployed radio cells keep shrinking. Soon micro and pico cells will play a major role in wireless networks. The micro/pico cells will not only provide better frequency reuse and coverage, but also will reduce power consumption and size of the portable units. In the micro/pico cellular scenario large number of base stations are required. Complete base stations are expensive. Therefore, number of base stations can be replaced by a single base station and a number of radio access points. RoF is a viable technology to interconnect the radio access points of these micro/pico cells cost effectively.

## 1.0.2 RoF to Support Broadband Wireless

Wireless is also at the edge of a significant revolution. It is moving from voice centric communications multimedia services. Currently over 81.4% of wireless subscribers in Japan has 3G wireless Internet capability. Data rates of these service continue to increase and the bit-rate capability of the wireless network must follow it. Furthermore, reliability and the quality of service is much more essential for wireless data services than for voice services. To catch up with the need, network operators keep increasing their bit rates. With High Speed Downlink Packet Access (HSDPA) in 3.5G, up to 14 Mbps is supported over 5 MHz bandwidth.

There is an inherent inverse relationship between the length of the wireless link and its bandwidth. An additional advantage of the micro cellular arrangement is the short air interface. Short air interface reduces the multi path delay spread that results in low inter symbol interference. In addition, often a strong line of sight path is available between the transmitter and the receiver in microcells and the path loss is less. As a result, high-speed multimedia services are easily accommodated in microcells.

### 1.0.3 RoF for 4G Networks

The 4G networks promise, whopping 100 Mbps to 1 Gbps over 100 MHz bandwidth to address the huge expected demand. This poses a big challenge for wireless communication engineers. At extremely high bit rates, over 1 Gbps, the air has to be significantly shorter, because the RF power need to be transmitted is extremely high. This is going to be a major deign challenge for 4G network planners.

## 1.1 Scope of the thesis

In this thesis, we are going to discuss and outline several parameters and propose an architecture for an indoor communication system. The scope is to discuss the basic principles, to investigate and to evaluate the performance of the proposed architecture.

The goal of this thesis work is to analyze the COFDM-RoF communication system with multimode fibre profile index $\alpha$ and different impairments on both channels . In this thesis, the most important RF impairments are reviewed and a joint analysis of these impairments is presented. The performance is evaluated through a theoretical analysis and simulation.

## 1.2 Problem statement

Although RoF technology reduces the cost of the base station units, deployment of fibers still increases the cost of the system. Up to now, most of the proposed systems operate with expensive single-mode fibres. In this proposal, we present the effect of COFDM to the graded index multimode fibre response, and propose an effective usage of cost efficient GI

multimode fibre. GI multimode fibre can also be allocated for COFDM-RoF systems with reasonable fibre distances.

Therefore, in order to investigate the feasibility of the COFDM-RoF systems, we analyze the performance of wireless local area networks (WLANs) under multipath fading and optical imperfections. We chose IEEE 802.11a standard as our basis model for the wireless system.

## 1.3  Major contribution of the thesis

The major contribution of this thesis are:

- The downlink and uplink analysis of a coded orthogonal frequency divisional multiplexing based optical fibre based wireless access architecture that is designed to support the WLAN system. The analysis includes mathematical derivations and numerical results that quantify the performance of the architecture.

- The performance of COFDM for a multimode fibre profile including graded index $\alpha$ profile is assessed.

- The cyclic prefix (CP) for the COFDM symbols is shown to combat the dispersion of the multipath fibre as well as the multipath delay of the wireless channel.

Also, the COFDM-RoF model has been proposed as solution for bandwidth demand. The combination of two different types of modulation has been performed to provide high bit rate data and bandwidth in WLAN in particular control station and base station.

The uplink involves with the signal first propagated through the air interface and then the RoF link. The downlink involves with signal first propagated through the RoF link then the air interface. The air interface introduces linear impairments such as additive white gaussian noise, and multipath fading, while the RoF link introduces nonlinear impairments such as intermodulation product distortion, optical noises and optical fibre nonlinearities. The analysis accounts for the cumulative effects of all the impairments.

# 1.4   Organization of the thesis

This thesis is organized as follows:

In Chapter 2, literature review of OFDM based multimode radio-over-fibre system and an overview of OFDM system are given. The signal model and problems associated with OFDM transmission are discussed. Also, it provides a brief summary of losses in communication channel. In the wireless channel, path loss, multipath fading, and shadowing effect are different aspects of signal propagation in air. The cause and effect of each aspect is investigated.

Chapter 3 covers the basic optical fibre communication link, RF/Optical signal generation, transportation methods and optical noise. The optical channel which is the RoF link has several mechanisms that affect the performance of the proposal architecture. The mechanisms can be categorized as the nonlinear and noise mechanisms. The nonlinear mechanism includes the intermodulation product and $\alpha$ profile in optical fiber. The relative intensity noise, shot noise and thermal noise are the noise mechanisms. All the mechanisms are investigated in this chapter. The power loss involves the optical-to-electrical conversion, electrical-to-optical conversion and general fiber attenuation of the radio over fiber link is also discussed.

Chapter 4 presents the fiber based radio access architecture that supports the WLAN systems using COFDM technique in the optical channel. Using this technique, the WLAN signal transmits through a fiber-optic cable, is known as the RoF link. The downlink and uplink analysis are presented with mathematical derivations of the system performance.

The analysis is completed with the numerical results presented in Chapter 5. The results are graphical description of the performance of the proposed architectures. The results also leads to a discussion in this chapter.

Finally, conclusions and possible future research directions are discussed in Chapter 6.

# Chapter 2

# Literature Review and Basics

## 2.1 Radio-over-Fiber for Fi-Wi Systems

There is significant work done in the wireless access using the RoF link by many authors. Dixon et al. [4] has investigated the performance of different profile of multimode fibre over coded orthogonal frequency division multiplexing. They did comprehensive link-budget analysis and results shown that OFDM provide good protection against the frequency selectivity of a dispersive multimode fibre. Also, multimode fibre performed well over 10 km with optimum value. Fernando and Anpalagan [5] also studied the RoF link, and they have derived the cumulative SNR for the combination of the RoF link and the air interface. They also studied the relationship between the cumulative SNR and the SNR after the optical link. Matarneh et al. [6] carried out an experimental downlink work in time and frequency domain and investigated the performance of COFDM over multimode fibre in radio-over-fibre communication system. Moreover, measured the response of different segments of graded index MMF and many parameters were assessed in detail such as the effect of the fibre lengths, RMS delay spread, link gain, noise figure and AM-AM/AM-PM to investigated the link performance. Lee et al. [7] discussed the use of OFDM to counter the problem of multipath propagation in multimode fibres (MMF) and the simultaneous use of spectrally efficient modulation schemes such as quadrature amplitude modulation to increase the capacity of MMF transmission links. Also, experimentally showed that the potential of OFDM over MMF optical fibres. In the paper of Pizzinat, Urvoas, and Charbonnier [8] demonstrated the feasi-

bility of using low bandwidth MMF with MB-OFDM transmission for indoor radio-over-fibre communication system. They experimentally demonstrated the possibility of deploying very high data rates, UWB based multi-user home wireless network using low cast VCSEL and MMF. In the paper of Tabatabai and Al-Raweshidy [9] studied the performance of WLAN and ultra wide band (UWB) signals for indoor Rof system by using MMF with Mach Zehnder Interferometer (MZI) and concluded that RoF is able to support multiple services using low cost laser and MMF. In the invited paper, Armstrong [10] presented the introduction and feasibility of OFDM for optical communication system specially, for radio-over-fibre system. He highlighted the some aspects that are important in optical communication. Also, he described limitation which imposed by optical fibre nonlinearities and a new form of optical OFDM. In [11] Das et al., demonstrated experimentally the performance of MMF over RoF as low-cost alternative. They investigated performance of UMTS and WLAN signals through bi-directional link budget analysis and predicted ranges of such systems. The analysis indicated that good performance and signal coverage is possible with optimum design of indoor fibre-fed wireless systems, even when using such inexpensive components. In this paper [12] Gomes et al., used the pre-installed MMF and laser and described that better link performance is achievable with careful design when considering wireless path, and Mac protocol for WLAN. Because Mac protocol is affected by the fibre delay. Carlsson et al. [13] analyzed the single and multimode laser with SMF and MMF for RoF system. Moreover, compared the performance (dynamic range, link gain, noise figure (NF), and misalignment tolerance) of links with standard and high-bandwidth graded-index multimode fibres, with lengths up to 500 m, using directly modulated VCSELs as light sources. Also, analyzed the measured link gain, NF, and dynamic range in order to pinpoint major limitations and suggested modifications for improved link performance. The relative intensity noise in the RoF link is further improved by Fernando in [14] and this improved expression gives a more accurate model for the RoF link. In the paper by Kim and Chung [15], they had investigated several passive optical networks that support narrow band signal in microcellular communication system and they derived the carrier to noise and distortion ratio for the network. Fan

et al. [16] investigated the employment of RoF link in microcellular personal communication system. They have included the fading and the co-channel interference of the air interface to improve their model. They had also compared the performance between the uplink and the downlink.

## 2.2   Introduction

Efficient spectrum allocation, which is the primary goal in the design of communication systems, has been achieved through the use of source coding and modulation techniques. Modulation refers to the process that transforms a baseband signal to a passband signal by employing a modulating signal. The main goal of a modulation scheme is to transfer the message signal through a radio channel while minimizing the effects of channel impairments and the use of the radio spectrum.

Thus, the utilization of a modulation technique that contributes to efficient use of the available bandwidth under hostile channel conditions is very important in communication systems. Different modulation techniques, which meet the stringent demands for protocols that are bandwidth efficient with minimal distortion and interference, have been suggested for the 4th generation (4G) standard. Orthogonal Frequency Division Multiplexing (OFDM) is a one of the candidates for modulation technique used in $4G$ protocol. Although OFDM has been around for more than 40 years, its popularity has increased recently. OFDM, also named as multi-carrier or discrete multitone modulation, is gaining importance since it supports efficient use of the radio spectrum while combating intercarrier interference (ICI) and intersymbol interference (ISI).

Efficient utilization of radio spectrum includes minimizing the space between the modulated signals while avoiding ICI. In practice, guard bands, which contribute to an inefficient use of radio spectrum, are placed between adjacent carriers. OFDM based systems overcome ICI by allowing the bandwidth of the modulated carriers to overlap without making the system subject to ICI. Moreover, high data rate transmission which requires small symbol periods contribute to ISI in a multipath environment. OFDM based systems support

high data rates with a long symbol duration which effectively eliminates ISI.

## 2.2.1    OFDM for Mobile Communications

Orthogonal Frequency Division Multiplexing (OFDM) is a communication technique which allows the communication channel to be divided into a number of equally spaced frequency bands. The orthogonal sub-carriers carry the transmitted information in specified bands. OFDM is a combination of modulation and multiple-access scheme which enables many users to utilize the same frequency band.

As a modulation technique, OFDM modulates the data onto the sub-channels by varying the sub-channel's phase and/or amplitude accordingly. Since the sub-channels are orthogonal in an OFDM based system, the spectrum of the sub-channels overlap without causing interference. An OFDM system splits the data stream into N parallel data streams, each at a rate 1/N of the original rate. Consequently, each symbol is mapped to a carrier at a unique frequency and combined together using the Inverse Fast Fourier Transform to produce the required time domain waveform.

OFDM can also be considered as a multiple-access technique since a single sub-channel or a group of sub-channels can be assigned to various users. The assignment of sub-channels to individual subscribers is controlled by the media access control (MAC) layer.

OFDM based wireless systems have been designed to transfer wideband data at data rates comparable to those of wired services. OFDM based systems support efficient data and voice transmission. In addition, these systems provide acceptable performance under wireless channels that are highly susceptible to interference.

Currently, OFDM is used in a number of commercial wired applications such as digital subscriber line (DSL). OFDM based systems have also been utilized in wireless applications such as television and radio broadcast. In addition, several fixed wireless systems and wireless local area networks have witnessed the employment of OFDM.

## 2.2.2 OFDM transmission on multimode fiber

Although the bandpass region of the multimode fibre is relatively flat with amplitude of 6 to 10 dB below the amplitude at zero frequency, it may not be possible to use this passband region to transmit a signal with large bit rate compared to 3-dB modal bandwidth. The deep nulls and variation of the amplitude of the frequency response of the multimode fibre within the transmission frequency can significantly degrade the output signal of the multimode fibre. Thus, leading to high BER at the receiver. It is seen from [3] that the probability density function of the amplitude response of the multimode fibre in the high frequency range is Rayleigh distributed and does not depend on the frequency. This property of the bandpass region of the multimode fibre is similar to the property of the channel in a wireless communications system, i.e., the fibre is a wideband frequency-selective channel.

The effect of having a wideband frequency selective channel for data transmission can be overcome by using orthogonal frequency division multiplexing (OFDM). This technique has been proposed and analyzed by many groups of researchers [26, 31]. In OFDM, the high data rate signal is divided into many small data rate signals. These small data rate signals are then transmitted via different subcarrier frequencies. By doing this the wideband frequency-selective channel is separated into a series of many narrowband frequency-nonselective channels. The main requirement of doing OFDM is the orthogonality between all OFDM signals in the frequency domain. That is, the spectrum of each OFDM signal should not interfere with the spectra of neighbouring OFDM signals. To have completely non-overlapping spectra, the required bandwidth of the system will then be large, i.e., less spectral efficiency.

To increase the spectral efficiency of the system, the signal spectra must be packed tightly. By doing this, very sharp filtering (which is very difficult to implement) is needed. Thus, more system complexity is required [25]. It is seen that using sharp filtering is not a good way to increase the spectral efficiency of an OFDM system.

Another technique is to make the individual spectra to be *sinc* functions. The subcarriers are put at the nulls of the neighbouring spectra. It is seen that the OFDM spectra are not

bandlimited but they can be separated by the baseband processing using discrete-Fourier transform (DFT) techniques [25, 30]. The detailed analysis of using DFT for OFDM system is given in [28, 29]. The applications of using OFDM with fiber optic transmissions have been shown in [30, 31]. OFDM was used in the subcarrier multiplexed fiber-optic video transmission as a digital transmission scheme of the hybrid AM/OFDM system [30].

Another example of using OFDM with a fiber-optic system is shown in [31]. The multimode fibre is used as an inexpensive cell feed in broad-band 60-GHz indoor picocellular systems. To overcome the effect of multipath fading in a wireless environment, OFDM is chosen to be the modulation scheme for the wireless transmission. However, to reduce the complexity required by the remote site, the signal modulation should be done at the central base office and sent from the central base office to the remote site via an optical fiber system.

Using multimode fibre as the medium instead of singlemode fibre can reduce the cost of implementing the optical fibre system. However, the problem of using multimode fibre as the medium is the effect of the modal dispersion in multimode fibre. OFDM is used to overcome the multipath problems in wireless systems. It might also be able to reduce the effect of frequency selectivity in the dispersive multimode fibre. It was shown in [31] that OFDM can offer good protection against the frequency selectivity of the dispersive multimode fibre. Thus, the seamless transition between the fiber and radio parts of the system with an inexpensive cost for the fibre part is possible.

It is seen that the key point for combating a wideband frequency-selective channel, similar to what occurs for high frequencies in multimode fibee, is to divide a high bit rate signal into many small bit rate signals and transmit these signals with different subcarriers. By doing this, the wideband frequency-selective channel is transformed into a series of narrowband non-selective channels. OFDM is applicable in the multimode fibre transmission in the high frequency region.

## 2.2.3   OFDM basic principle

OFDM is a multiplexing technique which divides the bandwidth into multiple frequency subcarriers. In OFDM, a high-bit-rate data stream is divided into N parallel lower bit rate streams. Then those streams are modulated and transmitted in separate subcarriers. The symbol duration on each subcarrier increases to $T = NTs$ . If $N$ is large enough to ensure that the symbol duration time exceeds the channel delay spread, $T >> 0$, then it reduces the inter symbol interference.

In the OFDM system, all subcarriers are orthogonal to each other. OFDM allows the spectrum of each subcarrier to overlap, and by selecting a special set of orthogonal carrier frequencies, high spectral efficiency can be achieved because the mutual influence among the orthogonal subcarriers can be avoided. The orthogonality also greatly simplifies the design of both transmitter and receiver.

Figure 2.1 describes four orthogonal carriers in the time domain. In this example, all the subcarriers have the same amplitude and same initial phase [48]. However, in practice, the subcarriers are modulated in different amplitude and phase. As can be seen from Figure 2.1, the orthogonality in the time domain means within an OFDM symbol period, all subcarriers have integer cycles and the numbers of the cycles between the channels differ by integer numbers.

In OFDM, a high-bit-rate data stream is divided into N parallel lower bit rate streams. Then those streams are modulated and transmitted in separate subcarriers. The symbol duration on each subcarrier increases to $T = NTs$ . If $N$ is large enough to ensure that the symbol duration time exceeds the channel delay spread, $T >> 0$, then it reduces the inter symbol interference [49].

## 2.3   Characteristics of OFDM Signal

The followings are the basic characteristics employed in the operation of OFDM:
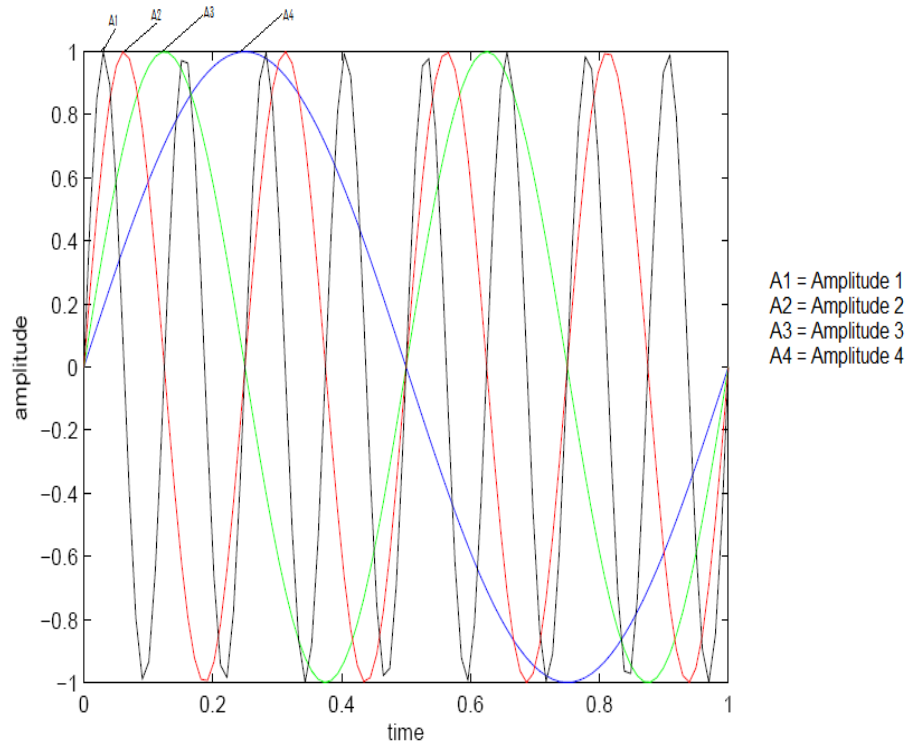
**Figure 2.1:** Orthogonal subcarriers in time domain

## 2.3.1 Orthogonality

The sub-carrier frequencies are chosen so that they are orthogonal to each other. This means that cross-talk between the sub-carriers is not possible and hence inter-carrier guard bands are not required. This orthogonality allows:

- Simultaneous transmission on numerous sub-carriers in a tight frequency band without interference from each other,

- High spectral efficiency, near the Nyquist rate,

- Simpler transmitter and receiver design,

- Efficient modulator and demodulator implementation using the FFT algorithm,

- Low complexity multiple access schemes such as coded orthogonal frequency division multiple access,

However, in order to maintain orthogonality, very accurate frequency synchronization is required between the receiver and the transmitter. If the frequency deviates, the sub-carriers would not remain orthogonal causing inter-carrier interference [64].

### 2.3.2 Guard Interval

OFDM transmits a number of low-rate streams in parallel instead of a single high-rate stream. Lower symbol rate modulation means the symbol duration is comparatively longer and it is feasible to insert a guard interval between OFDM symbols. The presence of this guard interval makes the system resilient to multi-path components and helps eliminate inter-symbol interference (ISI). The guard interval also eliminates the need for a pulse-shaping filter and reduces the sensitivity to time synchronization problems [65].

### 2.3.3 Cyclic Prefix

The cyclic prefix is transmitted during the guard interval and it consists of the end of the OFDM symbol copied into the guard interval. The cyclic prefix is transmitted followed by the OFDM symbol. Cyclic Prefix insertion is shown in Figure 2.2 [65]. The reason for the cyclic prefix being a copy of the OFDM symbols tail is so that the receiver will integrate over an integer number of sinusoid cycles for each of the multi-path components when it performs OFDM demodulation with the FFT.

### 2.3.4 Channel Coding and Interleaving

OFDM is invariably used in conjunction with channel coding (forward error correction), and almost always uses frequency and/or time interleaving. Frequency interleaving ensures that bit errors resulting from those sub-carriers that are selectively fading are spread out in the bit stream rather than being concentrated. This increases resistance to frequency-selective channel conditions. Similarly time interleaving ensures that bits close together in the bit
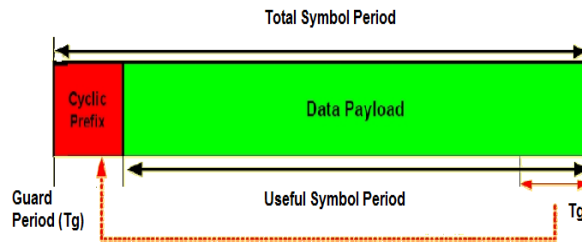
**Figure 2.2:** Insertion of Cyclic Prefix

stream are transmitted further apart in time, thus mitigating against severe fading, as would happen at high speeds. Common types of error correction coding used with OFDM-based systems are convolutional coding, Reed-Solomon coding and turbo coding. Error correction coding is employed in the receiver to correct any errors that result from environmental effects [65].

## 2.4 Coded OFDM

By using time and frequency diversity OFDM provides a means to transmit data in a frequency selective channel. However, it does not suppress fading itself. Depending on their position in the frequency domain, individual subchannels could be affected by fading. This requires the use of channel coding to further protect transmitted data. Among those channel coding techniques, convolution coding combined with frequency and time interleaving is considered the most effective means for a frequency selective fading channel.

Coded OFDM (COFDM) is OFDM that makes use of interleaving and forward error correction (FEC) coding for protection of data against errors. Error correction coding provides redundancy to the signal in order for the receiver to be able to correct any bits that are received in error. The error correction decoder in COFDM is the Viterbi algorithm which tries to decode what bits were sent based on the received sampled values.

COFDM also allows different groups of bits to be protected with a different strength code

rate. This is done in cases where some bits are more important for the correct reproduction of the signal than other bits, such as the filter parameters in MPEG audio streams. This allows the Viterbi error correction decoder a higher chance of correcting any errors [22].

It should be mentioned that one of the advantages of OFDM is that it can convert a wideband frequency selective fading channel into a series of narrowband and frequency non-selective fading subchannels by using parallel and multicarrier transmission. Coding OFDM subcarriers sequentially by using specially designed codes for frequency non-selective fading channel is the major reason for using COFDM for terrestrial broadcasting.

In general, transmission errors have a strong time/frequency correlation. Interleaving plays an essential role in channel coding by providing diversity in the time domain. Interleaving breaks the correlation and enables the decoder to eliminate or reduce local fading throughout the band and over the whole depth of the time interleaving. Interleaving depth should be large enough to break long straight errors.

Coded OFDM, or COFDM, is a term used for a system in which the error control coding and OFDM modulation processes work closely together. An important step in a COFDM system is to interleave and code the bits prior to the IFFT. This step serves the purpose of taking adjacent bits in the source data and spreading them out across multiple subcarriers. One or more subcarriers may be lost or impaired due to a frequency null, and this loss would cause a continuous stream of bit errors. Such a burst of errors would typically be hard to correct. The interleaving at the transmitter spreads out the continuous bits such that the bit errors become spaced far apart in time. This spacing makes it easier for the decoder to correct the errors. Another important step in a COFDM system is to use channel information from the equalizer to determine the reliability of the received bits. The values of the equalizer response are used to infer the strength of the received subcarriers. For example, if the equalizer response had a large value at a certain frequency, it would correspond to a frequency null at that point in the channel. The equalizer response would have a large value at that point because it is trying to compensate for the weak received signal. This reliability information is passed on to the decoding blocks so that they can properly weight the bits

when making decoding decisions. In the case of frequency null, the bits would be marked as "low confidence".

## 2.5 COFDM Performance Expectation

### 2.5.1 Multipath/fading

It is believed that with properly designed guard interval, interleaving and channel coding, COFDM is capable of handling very strong echoes. The BER improvement resulted from multiple echoes was indicated by the computer simulations. With the assumption of withstanding strong multipath propagation, COFDM might allow the use of omni-directional antenna in urban areas and mobile reception where C/N is sufficiently high. In addition to channel fading, time-variant signals caused by transmitter tower swaying, airplane fluttering and even tree swaying generate dynamic ghosts and consequently produce errors in digital transmission. With its parallel transmission structure as well as the use of trellis coding, COFDM systems might present advantages in fading and time-variant channel environment.

### 2.5.2 Impulse Interference

COFDM is more immune to impulse noise than a single carrier system because a COFDM signal is integrated over a long symbol period and the impact of impulse noise is much less than that for single carrier systems. As a matter of fact, the immunity of impulse noise was one of the original motivations for MCM. Studies indicated that the best approach of impulse noise reduction for OFDM involves a combination of soft and hard error protection.

### 2.5.3 Peak-to-average Power Ratio

The peak-to-average power ratio for a single carrier system depends on the signal constellation and the roll-off factor of pulse shaping filter (Gibbs' phenomenon). Theoretically, the difference of the peak-to-average power ratio between a multicarrier system and a single carrier system is an function of the number of carriers as:

$$\Delta(dB) = 10 \log_{10} N$$

where, N is the number of carriers. When N = 1000, the difference could be $30dB$. However, this theoretical value can rarely occur. Since the input data is well scrambled, the chances of reaching its maximum value are very low, especially when the signal constellation size is large.

Since COFDM signal can be treated as a series of independent and identically distributed carriers, the Central Limit theorem implies that the COFDM signal distribution should tend to be Gaussian when the number of carriers, N, is large. Generally, when N > 20, which is the case for most of the COFDM systems, the distribution is very close to Gaussian. Its probability of above three times (9.6 dB peak-to- average power ratio) of its variance, or average power, is about 0.1%. For four times of variance, or 12 dB peak-to-average power ratio, it is less than 0.01%.

It should be pointed out that, for each COFDM subchannel, there is usually no pulse shaping implemented. The peak-to-average power ratio for each subchannel depends only on the signal constellation. In common practice, signals could be clipped because of limited quantization levels, rounding and truncation during the FFT computation as well as other distributed parameters after D/A conversion. It is safe to say that the Gaussian model can be used as the upper bound for COFDM signals.

### 2.5.4 Nonlinear Distortion

Since the broadcast transmitter is a nonlinear device, clipping will always happen for COFDM signal. However, clipping of a COFDM signal is similar to the impulse interference on which COFDM systems have strong immunity.

## 2.6 Losses in Communication Channel

### 2.6.1 Communication Channel

Channel in the communications refers to the medium through which information is transmitted from a sender or transmitter to a receiver. In practice, this can mean many different methods of facilitating communication, including:

- A connection between initiating and terminating needs of a circuit,

- A path for conveying RF signals, usually distinguished from other parallel paths,

- In a communication system, the part that connects a data source to a data sink.

## 2.6.2   Path Loss

The RF power loss in air is expressed as a function of distance between MSs and the RAP. It is modeled as a large-scale propagation model. The expression for a received signal power in [42] is given as follows:

$$P_r = S \, P_t \left( \frac{\lambda}{4 \, \pi \, r} \right)^{\gamma} \tag{2.1}$$

where, $P_r$ is the received signal power, $P_t$ is the transmitted signal power, $S$ is the parameter that reflects the shadowing effect, $\lambda$ is the wavelength of the transmitted signal, $r$ is the distance from the MS to the base station, and $\gamma$ is the path loss exponent. The expression is modified to express as a function of a received RF power loss to a 90% confidence coverage radius. This expression gives the statistical signal attenuation for a distance between the MS and the base station. The distance is said to be 90% confidence coverage radius which means the attenuation at that distance does not exceed the calculated value for 90% of the time. The modified expression is given as follows:

$$L_{wl}(R_{90}) = \frac{1}{S} \left( \frac{4\pi R_{90}}{\lambda \, 10^{\left( \frac{-0.13\sigma}{\gamma} \right)}} \right)^{\gamma} \tag{2.2}$$

where, $R_{90}$ is the 90% confidence coverage radius. The term $10^{\left( \frac{-0.13\sigma}{\gamma} \right)}$ comes from the relationship between the 90% confidence coverage radius $R_{90}$ and the average coverage radius $r$ [52], where, $\sigma$ and $\gamma$ are the standard deviation of the channel loss and the path loss exponent respectively.

## 2.6.3   Noise

In communication systems, the unwanted signal that corrupts the transmitted signal is referred to as noise. The undesirable effects imposed by noise on the transmitted message bits results in limiting the rate at which the data is transmitted. Thermal noise is referred to as the prominent noise source in communication systems. Thermal noise is described as a zero mean Gaussian random process. A Gaussian process $n(t)$ is a random function whose value $n$ at any arbitrary time t is identified by the Gaussian probability density function. Gaussian Noise is a theoretical frequency distribution for a set of variable data [50].

## 2.6.4   Additive White Gaussian Noise

In communication systems, thermal noise is modeled as Additive White Gaussian noise (AWGN). White noise is characterized of having a frequency spectrum that is continuous and uniform over a specified frequency band. Since white noise has a uniform spectral, it has the same power density for all frequencies [54]. The autocorrelation function of white noise, which is indicated in the following equation, is determined by using the inverse Fourier transform of the noise power spectral density.

$$R_n(\tau) = F^{-1}\{G_n(f)\} = \frac{No}{2}\delta(\tau) \tag{2.3}$$

According to the above equation, samples of white noise for a given noise signal $n(t)$ is uncorrelated from its time-shifted versions. The autocorrelation of white noise, which is a delta function, is indicated in Figure 2.3. Since white noise consists of uncorrelated samples, the noise samples are random.

Hence, a channel that is characterized with AWGN corrupts the transmitted symbols in a random manner. The only impairment in AWGN channel is the linear addition of wideband gaussian noise with a constant spectral density. Consequently, these channels does not impose fading, frequency selectivity, nonlinearity or dispersion.
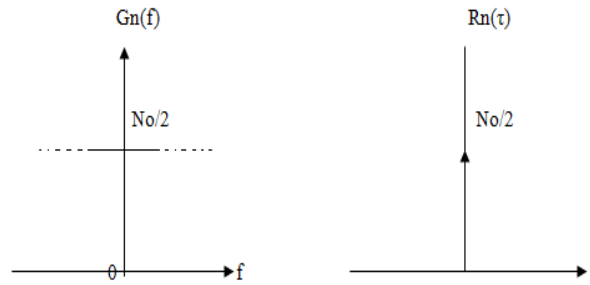
**Figure 2.3:** Autocorrelation of white noise

## 2.7 Multipath Fading

Multipath fading occurs when two or more delayed version of the transmitted signal creates interference due to reflection and scattering. As shown in Figure 2.4, the effect is significant because over a small travel distance or time interval the signal strength can change rapidly. At the receiver where the received signal is the summation of the delayed version of the signal, time dispersion or inter-symbol interference (ISI) is created. The ISI reduces the data rate that can be transmitted. Whenever surrounding objects or the mobile station are moving at a fast pace, the received signal would appear to have random frequency modulation. This effect is known as Doppler shift.
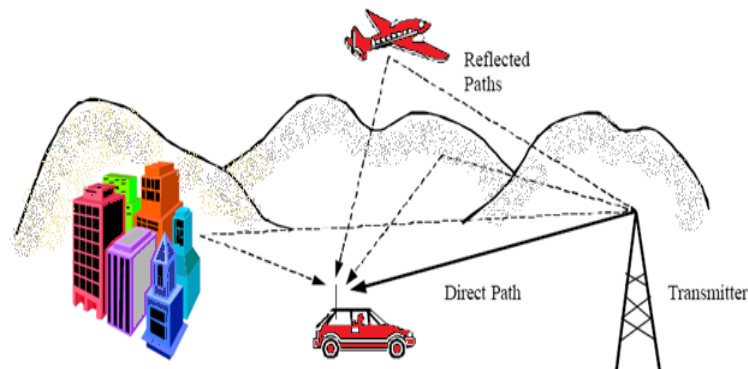


**Figure 2.4:** Multipath fading signals

Due to the random nature of the wireless channel, a statistic model of the channel can be obtained with an ensemble of many measurements took from a local area. A baseband equivalent of the multipath fading channel is given in [55] as follows:

$$h_b(t, \tau) = \sum_{i=1}^{L} a_i(t) \exp\left(-j\theta_i(t)\right) \delta(t - \tau_i(t)) \tag{2.4}$$

where, $L$ is the number of resolvable signal path, $a_i(t)$ is the amplitude, $\theta_i(t)$ is the amplitude or phase shift, and $\tau_i(t)$ is the time delay of individual path. It can be seen from the fading channel expression that the signal envelop is time variant, but angle and time delay are dependent on time.

In the context of this thesis, it is expected that the mobility within the cell is lower which means the Doppler spread profile of the channel is quite relaxed. The assumption for such a wireless channel is a frequency selective and a slow fading one. With slow fading, the channel can be assumed to remain invariant for at least few symbol periods. The impulse response of the fading channel (2.4) can be rewritten as follows:

$$h_b(\tau) = \sum_{i=1}^{L} a_i \exp\left(-j\theta_i\right) \delta(t - \tau_i) \tag{2.5}$$

A frequency selective channel is related to the delay spread profile of the channel and the transmitted bandwidth. When a transmitted bandwidth is much greater than the coherent bandwidth, the signal is said to experience frequency selective fading. It has been reported in [56] that for the 2 GHz spectrum the delay spread in urban propagation environment have an average of 1.1 $\mu$s for 90% of time and a maximum delay spread of 11 $\mu$s. These delay spread parameters translate to a coherent bandwidth in kHz range. The bandwidth of the two systems is in the MHz range.

## 2.8 Summary

In this chapter, we have described the literature review of multimode fibre over radio-over-fibre communication system , basic of OFDM and its characteristics. OFDM is one of the candidates for future modulation technique and will be used in $4G$ network because of higher transmission rate with minimal distortion and interference. Also, this chapter discussed the losses in the air and explained important modeled as a large and small scale propagation model.

# Chapter 3

# Optical Link, Transmission methods and Nonlinearities

## 3.1 Introduction

Wireless networks based on RoF technologies have been proposed as a promising cost-effective solution to meet ever increasing user bandwidth and wireless demands. Since it was first demonstrated for cordless or mobile telephone service in 1990 [5], a lot of research has been carried out to investigate its limitation and develop new and high performance RoF technologies. In this network a central base station (CBS) is connected to numerous functionally simple radio access points (RAPs) via an optic fiber. The main function of RAP is to convert optical signal to wireless one and vice versa. Almost all processing steps including modulation, demodulation, coding, routing is performed at the CBS. That means, RoF networks use highly linear optic fiber links to distribute RF signals between the CBS and RAPs.

Figure 3.1 shows a general RoF architecture. At a minimum, an RoF link consists of all the hardware required to impose an RF signal on an optical carrier, the fibre-optic link, and the hardware required to recover the RF signal from the carrier. The optical carrier's wavelength is usually selected to coincide with either the 1.3 $\mu m$ window, at which standard single-mode fibre has minimum dispersion, or the 1.55 $\mu m$ window, at which its attenuation is minimum.

Optical Fiber

Control
Station
(CS)

BS

E/O

T/R

O/E

Base Station (BS)

E/O : Electric-to-Optic Converter
O/E : Optic-to-Electric Converter
T/R : Transmitter/Receiver
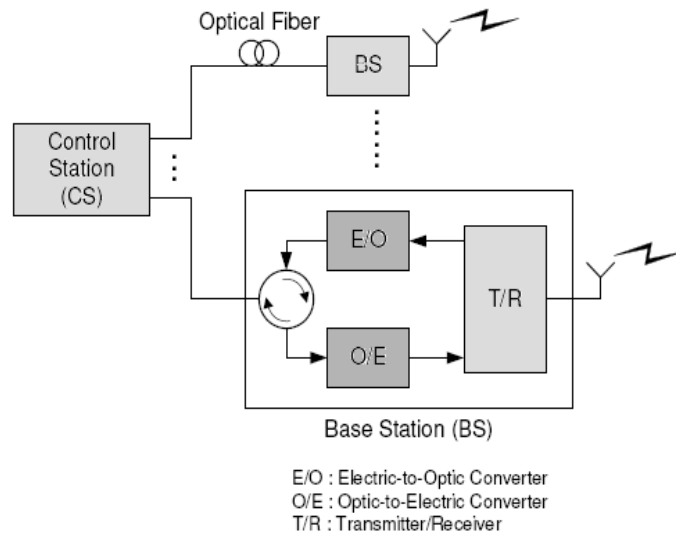
**Figure 3.1:** Basic RoF system

This chapter, constituting three major parts, briefly covers basic optical fibre transmission link, basic RF/Optical signal generation, transportation methods and optical noises. The first part is dedicated to a description of general optical transmission link, where digital signal transmission is assumed as current optical networks. The second part explains the radio and optical signal generation and transportation methods. The third part describes the most important noises in optical link.

## 3.2 Optical Transmission Link

In the first part of this section, a general optical transmission link , shown in Figure 3.2, is briefly described for which we assume that a digital pulse signal is transmitted over optical fibre unless otherwise specified. The optical link consists of an optical fibre, transmitter, receiver and amplifier, each of which is dealt with in the subsequent subsections.
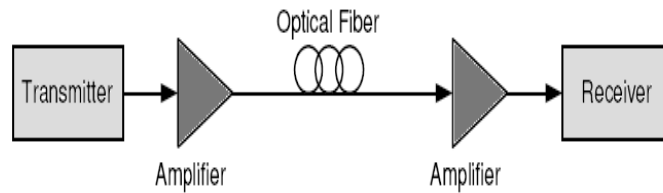
**Figure 3.2:** Optical transmission link

## 3.2.1   Optical Fibre

Optical fibre is a dielectric medium for carrying information from one point to another in the form of light. Unlike the copper form of transmission, the optical fibre is not electrical in nature. To be more specific, fibre is essentially a thin filament of glass that acts as a waveguide. A waveguide is a physical medium or path that allows the propagation of electromagnetic waves, such as light. Due to the physical phenomenon of total internal reflection, light can propagate following the length of a fibre with little loss (Figure 3.4).

Optical fibre has two low-attenuation regions [35]. Centered at approximately 1300 $nm$ is a range of 200 $nm$ in which attenuation is less than 0.5 $dB/km$. The total bandwidth in this region is about 25 THz. Centered at 1550 $nm$ is a region of similar size with attenuation as low as 0.2 $dB/km$. Combined, these two regions provide a theoretical upper bound of 50 THz of bandwidth. By using these large low-attenuation areas for data transmission, the signal loss for a set of one or more wavelengths can be made very small, thus reducing the number of amplifiers and repeaters actually needed. In single channel long-distance experiments, optical signals have been sent over hundreds of kilometers without amplification. Besides its enormous bandwidth and low attenuation, fibre also offers low error rates. Communication systems using an optical fibre typically operate at BER's of less than $10^{-11}$. The small size and thickness of fibre allow more fiber to occupy the same physical space as copper,

a property that is desirable when installing local networks in buildings. Fiber is flexible, reliable in corrosive environments, and deployable at short notice. Also, fiber transmission is immune to electromagnetic interference and does not cause interference.

## 3.2.2   Optical Transmission in Fibre

Light can travel through any transparent material, but the speed of light will be slower in the material than in a vacuum. The ratio of the speed of light in a vacuum to that in a material is known as the *material's refractive index (n)* and is given by $n = c/v$, where $c$ is the speed in a vacuum and $v$ is the speed in the material. When light travels from one material of a given refractive index to another material of a different refractive index (i.e., when refraction occurs), the angle at which the light is transmitted in the second material depends on the refractive indices of the two materials as well as the angle at which light strikes the interface between the two materials. According to Snell's law, we have $n_a \, sin\theta_a = n_b \, sin\theta_b$, where $n_a$ and $n_b$ are the refractive indices of the first substance and the second substance, respectively; and $\theta_a$ and $\theta_b$ are the angles from the normal of the incident and refracted lights, respectively.

From Figure 3.3, we see that the fiber consists of a core completely surrounded by a cladding (both of which consist of glass of different refractive indices). Let us first consider a step-index fibre, in which the change of refractive index at the core-cladding boundary is a step function. If the refractive index of the cladding is less than that of the core, then the *total internal reflection* can occur in the core and light can propagate through the fibre as shown in Figure 3.4. The angle above which total internal reflection will take place is known as the critical angle and is given by $\theta_c$,

$$\sin \theta_c = \frac{n_{clad}}{n_{core}},$$

where, $n_{clad}$ and $n_{core}$ are the refractive indices of cladding and core, respectively. Thus, for a light to travel down a fiber, the light must be incident on the core-cladding surface at an angle greater than $\theta_c$.

For the light to enter a fibre, the incoming light should be at an angle such that the refraction at the air-core boundary results in the transmitted light's being at an angle for

which total internal reflection can take place at the core-cladding boundary. The maximum value of $\theta_{air}$ can be derived from,

$$n_{air} \sin \theta_{air} = n_{core} \sin(90^o - \theta_c).$$

We can rewrite it as,

$$n_{air} \sin \theta_{air} = \sqrt{n_{core}^2 - n_{clad}^2} \; .$$

The quantity $n_{air} \sin \theta_{air}$ is referred to as the *numerical aperture* (NA) of the fibre and $\theta_{air}$ is the maximum angle with respect to the normal at the air-core boundary, so that the incident light that enters the core will experience total internal reflection inside the fibre.
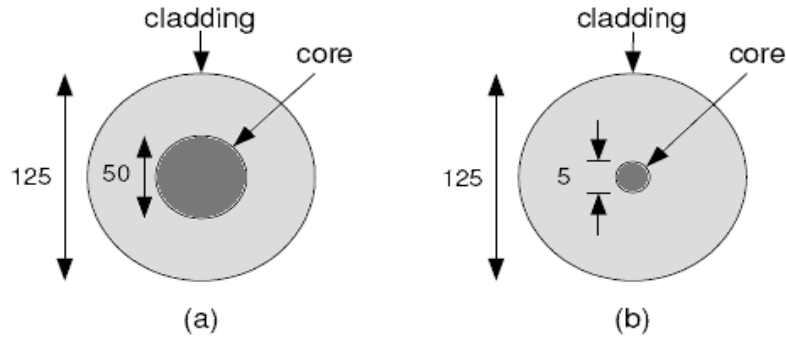


**Figure 3.3:** Multimode (a) and single-mode (b) optical fibres

## 3.2.3  Multi-mode versus Single-Mode Fibre

A mode in an optical fibre corresponds to one of the possible multiple ways in which a wave may propagate through the fibre. It can also be viewed as a standing wave in the transverse plane of the fibre. More formally, a mode corresponds to a solution of the wave equation that is derived from Maxwell's equations and subject to boundary conditions imposed by the optical fibre waveguide.
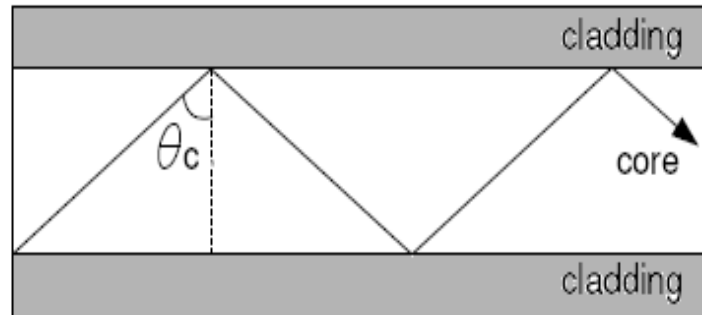
**Figure 3.4:** Light traveling via total internal reflection within an optical fibre

Although total internal reflection may occur for any angle $\theta$ that is greater than $\theta_c$, light will not necessarily propagate for all of these angles. For some of these angles, light will not propagate due to destructive interference between the incident light and the reflected light at the core-cladding interface within the fibre. For other angles of incidence, the incident wave and the reflected wave at the core-cladding interface constructively interfere in order to maintain the propagation of the wave. The angles for which waves do propagate correspond to modes in a fibre. If more than one mode propagates through a fibre, then the fibre is called multi-mode. In general, a larger core diameter or high operating frequency allows a greater number of modes to propagate.

The advantage of multi-mode fibre is that, its core diameter is relatively large; as a result, injection of light into the fibre with low coupling loss can be accomplished by using inexpensive, large-area light sources, such as light-emitting diodes (LED's). It's less sensitive for microbending and macrobending , and used for data center wiring specially for LAN installation. Multi-mode optical cable has a larger diameter and can be used to carry signal over short distances. Therefore, high-speed networking standards like Gigabit Ethernet, Fibre Channel and 10 Gigabit Ethernet all include the MMF as a transmission media.

Single-mode fibre allows only one mode and usually has a core size of about 10 $\mu m$, while

multi-mode fiber typically has a core size of 50-100 $\mu m$. It eliminates intermodal dispersion and hence can support transmission over much longer distances. However, it introduces the problem of concentrating enough power into a very small core. LED's cannot couple enough light into a single-mode fibre to facilitate long-distance communications. Such a high concentration of light energy may be provided by a semiconductor laser, which can generate a narrow beam of light. Single-mode fibre optic components and devices are also more expensive than their counterparts multi-mode fibre. Multi-mode fibre is widely used in systems where low cost connections and distances and transmission speeds must be taken are used modestly.

There are many advantages in using fibre optic cable instead of copper cable. One advantage is that fibre cables support longer cable runs than copper. In addition, data is transmitted at greater speeds and higher bandwidths than over copper cables.

## 3.3 Core refractive index profile ($\alpha$) in GI multimode fibre

When the light is coupled into a fibre link, depending on the refractive index, the size of the fiber, and the angle of coupling, a number of different modes exists. Each mode in the fiber travels with a different velocity. As a result, pulse broadening occurs analogous to the delay spread in the wireless channels [57].

For some specific design parameters, only single mode of light is transmitted through the fiber core. Hence, resulting in single mode fibers, which do not have modal dispersion (or multi-mode pulse broadening). Although single mode fiber comes with high performance and much less pulse spread, it is both expensive and fragile. For a network-wide usage it will increase the cost to unreasonably high levels (still more than 99.5 per cent of all fibers deployed in the U.S. are multi-mode fibers) [58]. In this thesis, we investigate the system performance over multimode fibers as a low cost alternative.

Multimode fibers are cheap, easy to handle and widely deployed in the field. There are mainly two important kinds of dispersion mechanisms in fibers: material and modal

dispersion [57].

1) Material Dispersion: The index of refraction of a material is dependent on the wavelength, so each frequency component of light actually travels at a slightly different speed. As the distance increases, the pulse becomes broader, resulting material dispersion. In multimode fibers, material dispersion is very small compared to modal dispersion [59], so we will neglect this effect in our work.

2) Modal Dispersion: There are mainly two types of multimode fibers: step index and graded-core index [57]. The graded core index is the second generation optical fibers, developed for canceling most of the pulse spread with gradually changing the core index of the fiber according to a profile, the most popular one being $\alpha$-profile [59].

An optical impulse having a delta function waveform is launched into the fiber at the transmitting end. This impulse arrives at the receiving end after being widened by the multimode dispersion. In [59] more information about $\alpha$-profile multimode fibers is given and the impulse response is formulated. In our simulations, the fiber impulse response given in [60] is derived as:

$$h_{MMF}(t) = \left\{ \begin{array}{ll} \frac{\alpha+2}{\alpha} |\frac{\alpha+2}{\Delta(\alpha-2)}|^{(2/\alpha)+1} |t|^{2/\alpha} & except\ for\ \alpha \neq 2 \\ \\ \frac{2}{\Delta^2} & for\ \alpha \approx 2 \end{array} \right\} \tag{3.1}$$

Time $t$ changes for 0 to $T$;

$$T = \left\{ \begin{array}{ll} \frac{\alpha-2}{\alpha+2}\Delta & except\ for\ \alpha \neq 2 \\ \\ \Delta^2/2 & for\ \alpha \approx 2 \end{array} \right\} \tag{3.2}$$

where, $T$ is the delay difference between modes or multimode dispersion or intermodal delay dispersion.

# 3.4 Radio-over-Fiber Transportation Methods

Connecting relatively large numbers of RAPs to the Central Office is an issue that needs to be addressed. Optical fibre is the best medium because of its abundant bandwidth and low distortion properties. The optical signal is inherently immune to electromagnetic interference. Furthermore, in contrast to co-axial cables, every additional kilometer length of fibre increases the loss by only about one dB. These factors make the fibre the most attractive solution in interconnecting these wideband pico cells.

There are several advantages with radio-over-fibre transmission. Most importantly, high-speed A/D and D/A conversion requirements are eliminated because the RF signal can be used as it is. Besides, analog optical fibre links have the ability to transmit radio waves up to tens of GHz without any format conversion. Furthermore, when there are multiple RF carriers, they all can simply be summed and used to modulate a single optical carrier. In this way, all the RF carriers can be simultaneously transmitted via the fibre in a subcarrier multiplexed way.

In addition, microwave signals can even be optically processed. New techniques such as Fibre Bragg gratings enable RF signals to be filtered and tuned optically. This makes the RoF approach more attractive and opens new possibilities.

Essentially, three different methods exist for the transmission of RF signal over optical links with intensity modulation: (i) direct intensity modulation, (ii) External modulation, and (iii) remote heterodyning. In direct intensity modulation an electrical parameter of the light source is modulated by the information-bearing RF signal. In practical links, this is the current of the laser diode, serving as the optical transmitter. The second method applies an unmodulated light source and an external light intensity modulator. This technique is called an external modulation. In a third method, RF signals are optically generated via remote heterodyning, i.e., a method in which more than one optical signal is generated by the light source, one of which is modulated by the information-bearing signal and these are mixed or heterodyned by the photodetector or by an external mixer to form the output RF signal. In this thesis, we consider only direct intensity modulation.

Direct intensity modulation is the simplest of the three solutions. So it is used everywhere that it can be used. When it is combined with direct detection using PD, it is frequently referred to as intensity-modulation direct-detection (IMDD) (Fig. 3.5). A direct modulation link is so named because a semiconductor laser directly converts a small-signal modulation (around a bias point set by a dc current) into a corresponding small-signal modulation of the intensity of photons emitted (around the average intensity at the bias point). Thus, a single device serves as both the optical source and the RF/optical modulator (Fig. 3.5). One limiting phenomenon to its use is the modulation bandwidth of the laser. Relatively simple lasers can be modulated to frequencies of several GHz.
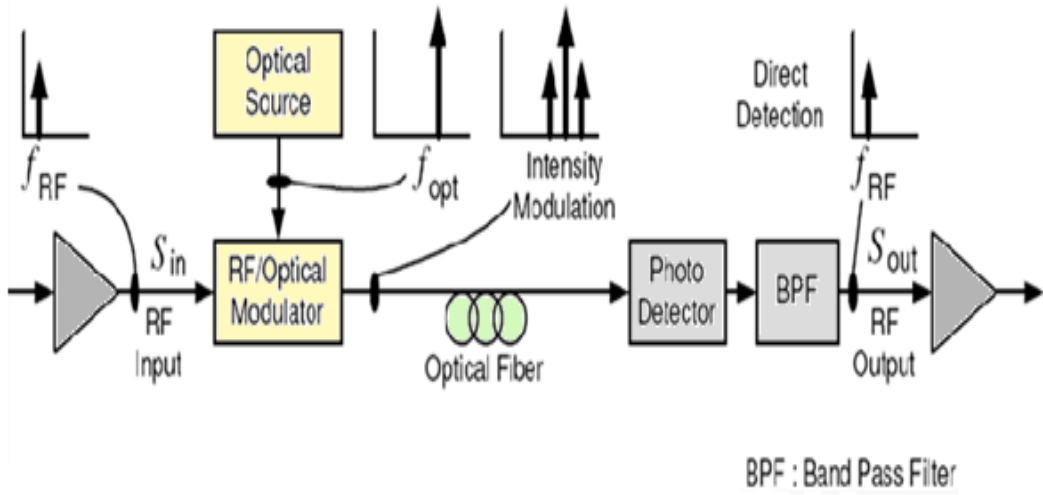


**Figure 3.5:** Intensity-modulation direct-detection (IMDD) optical link

## 3.5 RoF Link Configurations

In this section we discuss a typical RoF link configuration, which is classified based on the kinds of frequency bands transmitted over an optical fibre link. Representative RoF link configurations are schematically shown in Fig. 3.6.

Without light source for uplink transmission. In each configuration of the figure, RAPs do
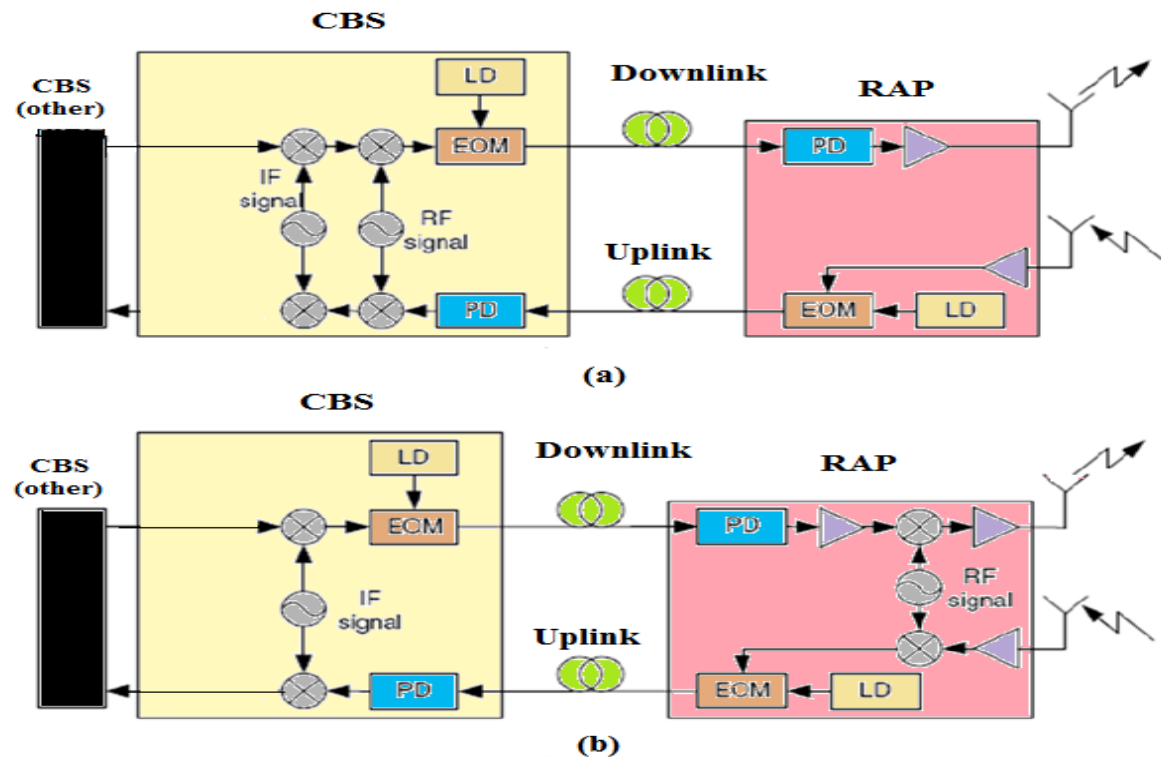
**Figure 3.6:** Representative RoF link configurations: (a) EOM, RF modulated signal.(b) EOM, IF modulated signal

not have any equipment for modulation and demodulation, only the CBS has such equipment.

In the downlink from the CBS to the RAPs, the information signal from the Internet, or other CBS is fed into the modem in the CBS. The signal that is either RF, IF or BB bands modulates optical signal from LD. As described earlier, if the RF band is low, we can modulate the LD signal by the signal of the RF band directly. If the RF band is high, such as the mm-wave band, we sometimes need to use external optical modulators (EOMs), like electroabsorption ones. The modulated optical signal is transmitted to the RAPs via optical fibre. At the RAPs, the RF/IF/BB band signal is recovered to detect the modulated optical signal by using a PD. The recovered signal, which needs to be upconverted to RF band if IF or BB signal is transmitted, is transmitted to the MHs via the antennas of the RAPs. In the configuration shown in Fig. 3.6 (a), the modulated signal is generated at the CBS in an RF band and directly transmitted to the RAPs by an EOM, which is called RF-over-Fibre. At each RAP, the modulated signal is recovered by detecting the modulated optical signal with a PD and directly transmitted to the MHs. Signal distribution as RF-over-Fibre has the advantage of a simplified RAP design but is susceptible to fibre chromatic dispersion that severely limits the transmission distance. In the configuration shown in Fig. 3.6 (b), the modulated signal is generated at the CBS in an IF band and transmitted to the RAPs by an EOM, which is called IF-over-Fibre. At each RAP, the modulated signal is recovered by detecting the modulated optical signal with a PD, upconverted to an RF band, and transmitted to the MHs. In this scheme, the effect of fibre chromatic dispersion on the distribution of IF signals is much reduced, although antenna RAPs implemented for RoF system incorporating IF-over- Fibre transport require additional electronic hardware such as a mm-wave frequency LO for frequency up- and down conversion.

In the configuration (c) of the Fig. 3.7, the modulated signal is generated at the CBS in baseband and transmitted to the RAPs by an EOM, which is referred to as BB-over- Fibre. At each RAP, the modulated signal is recovered by detecting the modulated optical signal with a PD, upconverted to an RF band through an IF band or directly, and transmitted to the MHs. In the baseband transmission, influence of the fibre dispersion effect is negligible,
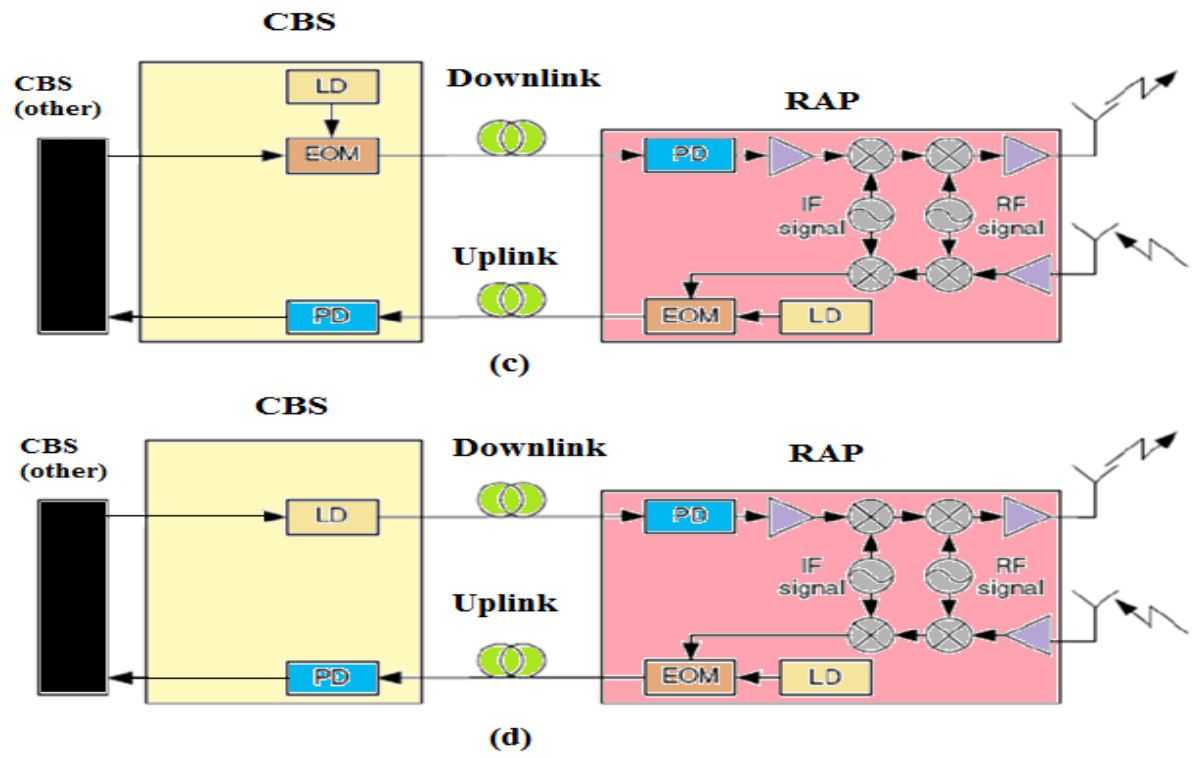
**Figure 3.7:** Representative RoF link configurations. (c) EOM, baseband modulated signal. (d) Direct modulation.

but the RAP configuration is the most complex. Since, without a subcarrier frequency, it has no choice but to adopt time-division or code division multiplexing. In the configuration shown in Fig. 3.7 (d), the modulated signal is generated at the CBS in a baseband or an IF band and transmitted to the RAPs by modulating a LD directly. At each RAP, the modulated signal is recovered by detecting the modulated optical signal with a PD, upconverted to an RF band, and transmitted to the MHs. This is feasible for relatively low frequencies, say, less than 10 GHz. By reducing the frequency band used to generate the modulated signal at the CBS such as IF over- Fibre or BB-over-Fibre, the bandwidth required for optical modulation can greatly be reduced. This is especially important when RoF at mmwave bands is combined with dense wavelength division multiplexing (DWDM). However, this increases the amount of equipment at the RAPs because an up converter for the downlink and a down converter for the uplink are required. In the RF subcarrier transmission, the RAP configuration can be simplified only if a mm-wave optical external modulator and a high-frequency PD are respectively applied to the electric-to-optic (E/O) and the optic-to-electric (O/E) converters. For the uplink from an MH to the CBS, the reverse process is performed.

In the configuration shown in Fig. 3.6 (a), the signals received at a RAP are amplified and directly transmitted to the CBS by modulating an optical signal from a LD by using an EOM. In the configuration (b) and (c), the signals received at a RAP are amplified and down converted to an IF or a baseband frequency and transmitted to the CBS by modulating an optical signal from a LD by using an EOM. In the configuration (d), the signals received at a RAP are amplified and down converted to an IF or a baseband frequency and transmitted to the CBS by directly modulating an optical signal from a LD.

## 3.6 Optical Noises

### 3.6.1 Quantum Noises

The shot or quantum noise arises from the random nature of the photons emitted from a laser diode and collected at a photodiode. The noise power of the shot noise is proportional

to the average received photocurrent $I_p = RP_o$ and the bandwidth $B$ of the modulated signal; it is given as [61]:

$$\langle i_{sh}^2 \rangle = \sigma_{sh}^2 = 2qI_pB \tag{3.3}$$

where, $q$ is the electron charge. For the average received photocurrent $I_p$, $\Re$ is the responsivity of the photodiode, and $P_o$ is the average optical power at the photodiode.

## 3.6.2 Relative Intensity Noise

The relative intensity noise (RIN) arises from the random nature of stimulated emission of a laser diode that results in fluctuation of the optical intensity. It is widely accepted that the power of this noise is proportional to the square of the received photocurrent, $I_p = \Re P_o$, and the RIN parameter. In [61], the RIN power is given as:

$$\langle i_{RIN}^2 \rangle = \sigma_{RIN}^2 = RIN \, I_p^2 \, B \tag{3.4}$$

where, $RIN$ is the RIN parameter, and $B$ is the bandwidth of the modulated signal. For the average received photocurrent $I_p$, $\Re$ is the responsivity of the photodiode, and $P_o$ is the average optical power at the photodiode.

The RIN parameter is defined as the ratio between the mean-square intensity fluctuation of a laser diode output optical power $\langle \Delta P^2(t) \rangle$ to the square of the mean optical power. It is measured in dB/Hz. This parameter depends on the temperature and the threshold current [24], but for commercial optical transmitter package the two factors are optimized. Therefore, the RIN parameter can simply be read off from a data sheet. Now, if we substitute the RIN parameter with the ratio, the square of the mean optical power is cancelled and the power of the RIN expression becomes:

$$\sigma_{RIN}^2 = \langle \Delta P^2(t) \rangle \, \Re^2 B \tag{3.5}$$

This expression shows the power of the RIN is independent from the mean optical power. The RIN also increases with the light reflection back to the laser diode [61]. However,

this reflection effect can be easily reduced by inserting an optical isolator in the optical transmitter.

The expressions (3.4) and (3.5) are also known as the intrinsic RIN which is accurate for a small optical modulation index ($m < 0.3$). However, for a large optical modulation index ($m > 0.3$), there is a sudden jump in RIN level. This additional RIN mechanism was investigated by Way in [62], and it is labeled as the dynamic RIN.

From experimental studies, it is clear that the dynamic RIN increases with the RF power of modulating signals to a laser diode. In [14], Fernando had derived an expression for the dynamic RIN that is independent of device parameters, and the expression agreed with Way's observation. He derived the expression with the following assumption. First, the optical power reaches the photodiode is given as:

$$P(t) = [1 + m\,s(t)][P_o + \Delta P(t)] \tag{3.6}$$

where, $m$ is the optical modulation index, $s(t)$ is the modulated signal, and $\Delta P(t)$ is the intensity fluctuation of a laser diode output optical power that reaches the photodiode. Then, the output photocurrent is assumed to go through an ideal bandpass filter with impulse response $h(t)$. The RIN power term is among the variance of the current, $\langle I_h^2(t) \rangle$, after the bandpass filter; and it is expressed as:

$$\langle I_h^2(t) \rangle = I_p^2\,m^2 \langle s^2(t) \rangle + \sigma_{sh}^2 + \sigma_{RIN}^2 \tag{3.7}$$

By removing the contribution of the modulated signal power and the shot noise, the RIN power is given as:

$$\sigma_{RIN}^2 = E\left[ \left\{ \Re \int_{-\infty}^{\infty} [1 + m\,s(\tau)]\,\Delta P(\tau)\,h(t - \tau)\,d\tau \right\}^2 \right] \tag{3.8}$$

From the above expression, we can see that the RIN power is independent of the average optical power $P_o$ and convolution is performed to determine the current output from the bandpass filter. After evaluating the expectation, the final RIN power expression is given as:

$$\langle i^2_{RIN} \rangle = \sigma^2_{RIN} = RIN \, I^2_p \, B \, (1 + \mu^2) \tag{3.9}$$

where, $\mu$ is the RMS optical modulation index. The RMS optical modulation index is proportional to the RF power of the modulated signal. Using the earlier assumptions, the RMS optical modulation index is $\sqrt{m^2 \langle s^2(t) \rangle}$.

### 3.6.3 Thermal Noise

The mean square value of the thermal noise is given by [61]:

$$\langle i^2_{th} \rangle = \sigma^2_{th} = \frac{4 \, k_B \, F \, T_o}{R_L} \tag{3.10}$$

where, $k_B$ is Boltzmann's constant, $T_o$ is the absolute temperature, $F$ is the amplifier noise figure and $R_L$ is the receiver resistance.

## 3.7   Summary

In this chapter a brief description of conventional optical transmission link, radio/optical signal generation, transportation methods, and basic optical components was given. Due to its potential to support broadband service with little infrastructure and many advantages such as cost-effectiveness, easy deployment, maintenance RoF networks will be a promising alternative to future wireless networks. Multi-mode fibre has higher "light-gathering" capacity than single-mode optical fibre. In practical terms, the larger core size simplifies connections and also allows the use of lower-cost electronics such as light-emitting diodes (LEDs) and vertical-cavity surface-emitting lasers (VCSELs) which operate at the 850 nm and 1300 nm wavelength (single-mode fibres used in telecommunications operate at 1310 or 1550 nm and require more expensive laser sources. Single mode fibres exist for nearly all visible wavelengths of light). The major impairments of the RoF link that limit the signal quality are the nonlinear distortion and various noise mechanisms were described in this chapter.

# Chapter 4

# Novel design of a Fibre-Wireless System Employing a COFDM Concept

In this chapter, we investigate the performance of coded orthogonal division multiplexing scheme that deploy the Fibre-Wireless link to provide wireless access to multiple users. The focus of this chapter is to study the downlink/uplink performance of COFDM Fibre-Wireless system and derived the general equations, to investigate the effect of various noise mechanisms of the Fibre-Wireless link, mainly the quantum (shot), thermal and relative intensity noise (RIN) mechanisms, to assess the $\alpha$ profile graded index fibre on COFDM, and the effect of cyclic prefix to the multimode fibre dispersion, in the OSNR performance, in addition to interference. Note that, of these noise mechanisms, quantum noise is function of the mean optical power while the RIN is a function of the instantaneous optical power. Therefore, the RIN increases with the modulating RF signal, while the shot noise relatively decreases with the modulation depth $m$. In addition to the above are the wireless channel additive noise, and multipath fading. Furthermore, the higher the RF signals bandwidth, the higher the noise power. However, the higher bandwidth is better at suppressing multiuser interference. All these factors introduce a quite complex situation that is investigated in this chapter.

# 4.1 Specifications of the Wireless LAN RoF System

The desired Fibre-Wireless system is required to be:

- Cost effective,

- Capable of operating within GIMMF modal bandwidth,

- Capable of transmitting BPSK modulated signals in multi-carrier systems such as in OFDM multiplexing,

- Easily upgradeable to operate at higher frequencies (mm-waves),

- Fulfil other requirements defined in the wireless LAN standard concerned.
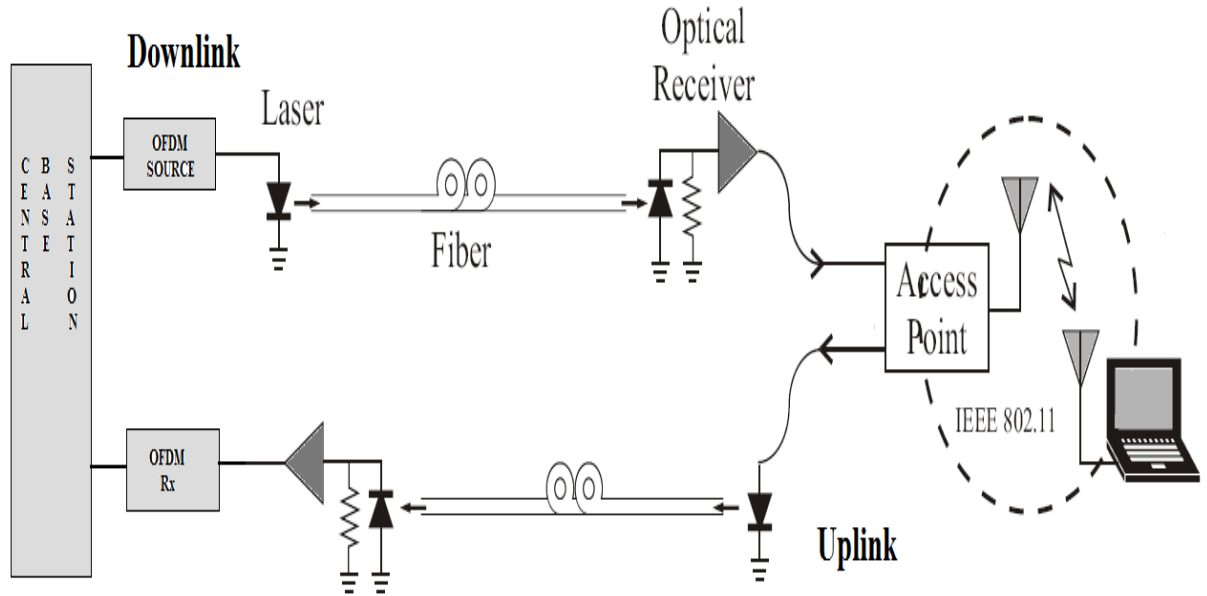


**Figure 4.1:** Proposed architecture of COFDM Fibre-Wireless communication system

The COFDM based RoF architecture supporting Wireless Local Area Networks (WLAN) is shown in Figure 4.1. In the downlink senario, the signal is transmitted from the central base station and first goes through the OFDM source, the radio-over-fibre link and then

through the air interface. In the uplink senario, the signal first propagated through the air interface and then the RoF link. The COFDM-RoF architecture consists of a OFDM source, directly modulated single longitudinal mode laser, graded index multi-mode fibre, and PIN photodiode optical receiver followed by an amplifier and an antenna.
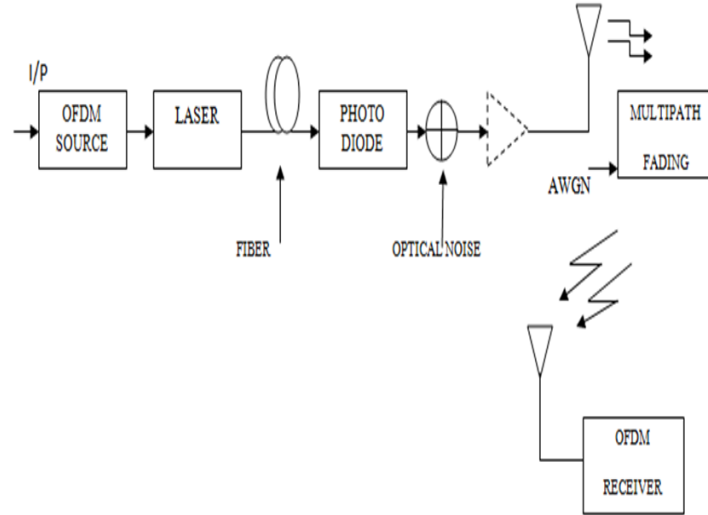


**Figure 4.2:** Simulated fibre-radio system block diagram

## 4.2   Downlink Analysis

In this section, we derive expressions for downlink, mainly the generation of OFDM signal, modulated laser optical signal, fibre nonlinearity with optimized impulse response, and the variances of optical link noise processes. These expressions are needed to evaluate the optical signal to noise ratio and cumulative signal to noise ratio that is done in the next section.

According to the Figure 4.3, the binary data is combined into symbols in accordance to the number of bits/symbol after protected by forward error correction (FEC) and interleaving. The type of error correction coding that is used here is convolutional coding. Error correction coding adds redundancy to the signal in order for the receiver to be able to correct any

bits that are received in error. Following, the serial symbol stream is converted into parallel segments according to the number of carriers. After that, the data is mapped through Binary Phase Shift Keying (BPSK) modulation scheme. Subsequent to application of modulation, an IFFT is performed to generate one symbol period in the time domain. Since OFDM modulation is applied in frequency domain, the IFFT of the signal is taken to change the signal to time domain. The size of the IFFT imposes a limit on the maximum number of carriers used by OFDM. OFDM carriers are defined in complex conjugate pairs to produce a real valued time signal. Consequently, the maximum number of carrier is equal to half the size of IFFT. After the IFFT, cyclic prefix is appended. Following, the parallel segments are converted back to the serial symbol stream before sent to the laser (also, as shown in Figure 4.2).
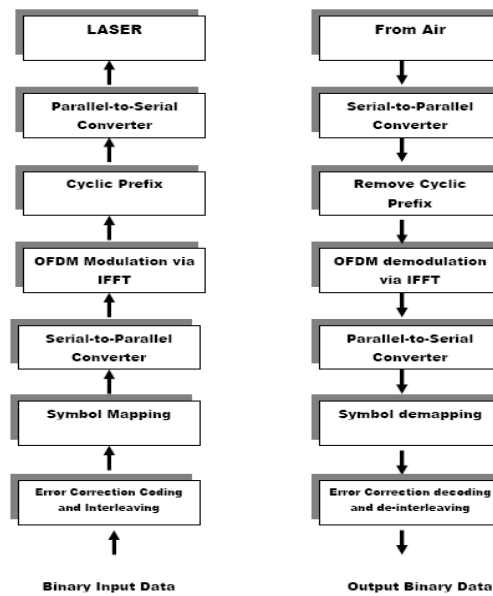
**Figure 4.3:** OFDM Transceiver block diagram

## 4.2.1 Optical Link Analysis

Lets assume that OFDM signal consists of $N$ subcarriers which are modulated by $a_{k,i}$ data symbol that are created by using BPSK modulation. For $i^{\text{th}}$ OFDM symbol, the signal is expressed as:

$$b_{n,i} = \frac{1}{N} \sum_{k=0}^{N-1} a_{k,i}(t) \, expj2\pi k \frac{(n - N_g)}{N} \tag{4.1}$$

Here, $a_{k,i}$ is the input data, $k = 0, 1, 2, 3, ....N - 1$, $b_{n,i}$ is the output data, $N$ is the number of data samples and $N_g$ is the cyclic prefix samples. This OFDM signal is directly modulated by the laser and converted into the optical signal. The laser output signal is given as:

$$s(t) = \frac{1}{N} \sum_{k=0}^{N-1} \sqrt{2P_{o,i}} \, a_{k,i}(t - \tau) \, expj2\pi k \frac{(n - N_g)}{N} \, \cos(\omega_\alpha t - \phi) \tag{4.2}$$

$$= \frac{1}{N} \sum_{k=0}^{N-1} A_i \, a_{k,i}(t - \tau) \, expj2\pi k \frac{(n - N_g)}{N} \, \cos(\omega_\alpha t - \phi) \tag{4.3}$$

where, $A_i$ is the optical signal power and equal to $\sqrt{2P_{o,i}}$, $\omega_\alpha$ is the laser carrier frequency, $\tau$ is the delay, $\phi$ is the phase, and $exp(j2\pi k \frac{(n - N_g)}{N})$ is the complex valued orthogonal subcarriers.

This optical signal is assumed noiseless because it is originated from the base station. Moreover, the optical signal is considered constant because the optical channel experiences no fading. Therefore, the RMS optical modulation index can be determined from the above expression and given by:

$$\mu = \sqrt{\frac{m^2}{2}}.$$

Then, the optical signal that comes from the laser, propagates through an optical fibre and experiences fiber attenuation. In the architecture under discussion in this thesis, we used multi-mode fibre for low cost and less fiber dispersion. For GI multi-mode fibre (MMF), the impulse response is derived by:

$$h_{MMF}(t) = \begin{cases} \frac{\alpha+2}{\alpha} |\frac{\alpha+2}{\Delta(\alpha-2)}|^{(2/\alpha)+1} |t|^{2/\alpha} & except\ for\ \alpha \neq 2 \\ \frac{2}{\Delta^2} & for\ \alpha \approx 2 \end{cases} \qquad (4.4)$$

Time $t$ changes for 0 to $T$;

$$T = \begin{cases} \frac{\alpha-2}{\alpha+2}\Delta & except\ for\ \alpha \neq 2 \\ \Delta^2/2 & for\ \alpha \approx 2 \end{cases} \qquad (4.5)$$

where, $\Delta$ is a function of refractive indexes of the core and the cladding mediums of the fiber and where $T$ is the delay difference between modes or multi-mode dispersion or intermodal delay dispersion. For all different $\alpha$ values, the total delay of the channel is normalized by the delay of the central mode. So, when $\alpha < 2$, the delay spread is shown negative since higher order modes arrive earlier than the central mode [60].

The optical signal that propagate through fibre from the base station to the radio access point experiences signal attenuation, optical noise and nonlinear distortion. These effects on the signal can be seen from the photocurrent output. At the end of RoF link, the photocurrent output can be expressed as:

$$i_D(t) = \frac{1}{N} \sum_{k=0}^{N-1} A_i\, a_{k,i}(t-\tau)\, expj2\pi k \frac{(n-N_g)}{N}\, \cos(\omega_\alpha t - \phi) * h_{MMF}(t) + n_{opt}(t) \qquad (4.6)$$

In the above equation, we didn't consider the laser nonlinearity. The signal experiences fiber attenuation and optical noises, where, $n_{opt}(t)$ is the optical noise. The $n_{opt}(t)$ is the time domain noise term in the RoF link. This noise consists of shot noise, RIN noise and thermal noise. The 'RIN' originates from the laser and it depends on the square of the photo diode current.

Therefore, $< n_{opt}^2 > =$ Shot noise + Thermal noise + RIN noise .

## 4.2.2   Optical Link Loss

The input RF signal not only undergoes electrical-to-optical-to-electrical (e-o-e) conversion, but also experiences other system losses such as optical connector loss, splitter loss, and splicing loss. These losses will add into a signal and referred to as total fibre loss or $F_{loss,dB}$.

Therefore, the total loss due to the RoF link, can be defined as:

$$F_{loss,dB} = F_{e/o} + F_{o/e} + F_{misc} \ ,$$

where, $F_{e/o}$, $F_{o/e}$, and $F_{misc}$ are losses due to electrical-to-optical conversion, optical-to-electrical conversion, connectors, splitters, and splices respectively.

Therefore, we can define the total loss:

$$F_{loss,dB} = 10 \log[\frac{Z_{in}}{G_m^2}] + 10 \log[\frac{\Re^2}{Z_{out}}] + n_c l_c \qquad (4.7)$$

or in another words, $\qquad F_{loss,dB} = 10^{(F_{loss,dB}/10)}.$

where, $Z_{in}$ is the input impedance of the laser transmitter (typically 50Ω), $Z_{out}$ is the impedance of photodiode (typically 50Ω), $G_m^2$ is the laser modulation gain (mW/mA), $\Re$ is the responsivity of photodiode, $n_c$ is the number of connectors, and $l_c$ is the connector loss.

Thus, the output of the photo diode produces a photo current that is proportional to the received optical power. Total detected current $i_D(t)$ is the sum of the mean (DC) current $I_D(t)$ and the ac component $i_d(t)$.

## 4.2.3   The Optical Signal to Noise Ratio

The complete optical signal to noise ratio (OSNR) of the RoF link considering the all dominant noise processes is given below:

$$OSNR = \frac{m^2\, I_D^2\, E[s^2(t)]\, F_{loss,dB}}{\langle n_{opt}^2(t)\rangle}. \tag{4.8}$$

The detected current $I_D$ is typically in milli-Amps range since the optical power in this application is in $mW$ range and the responsivity $\Re$ lies between zero and one $mA/mW$. Hence, the optical signal to noise ratio due to optical link noises is given by,

$$OSNR = \frac{m^2\, I_D^2\, E[s^2(t)]\, F_{loss,dB}}{RIN\, I_p^2\, B\,(1+\mu^2) + 2qI_pB + \frac{4\,k_B\,T_o}{R_L}}. \tag{4.9}$$

Typically, a RIN value is specified for a given laser diode in $dBm/Hz$, for example $-155dBm/Hz$.

## 4.2.4   Path Loss and Air Interference

Further analysis on the noise term $n(t)$ is necessary for a quantitative understanding of each noise mechanism. $n(t)$ consists of optical link noise terms $n_{opt}(t)$ as well as wireless link noise term $n_{wl}(t)$. The detected electrical signal at the optical receiver is weak and distorted by optical noise and needs to be amplified before radiated to the air. $n_{opt}(t)$ is amplified by optical post amplifier and undergoes wireless channel loss $L_{wl}$. Again, at the receiver, $n_{wl}(t)$ is added to the signal.

Therefore, the total noise including the noise in the air will be:

$$n(t) = \frac{n_{opt}(t)\, G_{opt}}{L_{wl}} + n_{wl}(t) \tag{4.10}$$

where, $G_{opt}$ is the optical post amplifier gain, $n_{wl}(t)$ is the wireless channel noise and $L_{wl}$ is the wireless channel loss.

From eqn.(4.10), wireless or optical link noise, may dominate the overall SNR. The optical link noise is composed of relative intensity noise (RIN), quantum noise and thermal noise. The wireless link noise composed of man made noise plus thermal noise.

According to the downlink communication, the signal that reaches the radio access point is then transmitted through air and received by users within the cell. The signal that propagates through air experiences path loss, fading and additive noise.

The path loss in air is modeled as a large scale propagation model. The model provides the average signal attenuation with a given distance away from the radio access point. The distance is said to be 90% confidence coverage radius which means that attenuation at that distance does not exceed the calculated value for 90% of the time.

## 4.2.5 Cumulative Signal to Noise Ratio

Assume, $r(t)$ is the received signal from the wireless channel. It is assumed the signal and noise are uncorrelated.

Therefore, the average power of received signal which is:

$$\langle r^2(t) \rangle = \langle r_s^2(t) \rangle + \langle r_n^2(t) \rangle$$

where, $\langle r_s^2(t) \rangle=$ signal power and $\langle r_n^2(t) \rangle=$ noise power

The cumulative SNR that accounts for path loss in the downlink is evaluated at the mobile station (MS). Therefore, with the assumption that the wireless and optical noises are uncorrelated, we can get the $SNR_c$ as given below:

$$SNR_c = \frac{m^2 I_D^2 \, F_{loss,dB} \left( \frac{G_{opt}^2}{L_{wl}^2} \right)}{\langle n_{opt}^2(t) \rangle \left( \frac{G_{opt}^2}{L_{wl}^2} \right) + \langle n_{wl}^2(t) \rangle}, \tag{4.11}$$

or in other words,

$$SNR_c, (dB) = OSNR - 10\log(1 + \frac{L_{wl}^2}{G_{opt}^2}). \tag{4.12}$$

## 4.3   Uplink Analysis

In the uplink of the architecture, RF signals are transmitted from multiple MSs and then they are received at the RAP. Let a subscript $\beta$ be an indication for the MS signal that belongs to the WLAN system.

$$s_{s,i}(t) = \frac{1}{N} \sum_{k=0}^{N-1} \sqrt{2P_{o,i}} \, a_{k,i}(t - \tau) \, expj2\pi k \frac{(n - N_g)}{N} \, \cos(\omega_\beta \, t) \tag{4.13}$$

$$s_{s,i}(t) = \frac{1}{N} \sum_{k=0}^{N-1} B_\beta \, a_{k,i}(t - \tau) \, expj2\pi k \frac{(n - N_g)}{N} \, \cos(\omega_\beta \, t) \tag{4.14}$$

where, $P_{o,i}$ is the received symbol power at the RAP, and $B_\beta$ is the Rayleigh distributed random variable of signal amplitude which $B_\beta = \sqrt{2P_{o,i}}$ , and the carrier frequency. Expression (4.13) illustrates the design of the WLAN system that only one MS can access the radio medium at a time. The WLAN system uses the 2.4 GHz band and occupies a larger bandwidth of 22 MHz. At the RAP, the received signal that consists of WLAN signals is given as:

$$s_{RAP}(t) = s_{s,i}(t - \tau_\beta) + n_{up,wl}(t), \tag{4.15}$$

$$= B_\beta \frac{1}{N} \sum_{k=0}^{N-1} B_\beta \, a_{k,i}(t - \tau_\beta) \, expj2\pi k \frac{(n - N_g)}{N} \, \cos(\omega_\beta t - \phi_\beta) + n_{up,wl}(t), \tag{4.16}$$

where, $\tau_\beta$ is the time delay, and $\phi_\beta = \omega_\beta \, \tau_\beta$ is the phase of signal which is related to the time delay, and $n_{up,wl}(t)$ is the additive white Gaussian noise in air. Due to cell coverage requirements, the WLAN signal experiences Rician fading in air. Rician fading has a line of sight component. In the analysis, system is assumed to be in a harsh wireless environment where it has no line of sight path. The multipath fading in the wireless environment is

described in section 2.5. The effect of path loss in the wireless environment is embedded in the signal amplitudes. The path loss has been discussed in section 2.4.2.

The delay $\tau_\beta$ is the combination of an access time to the system and a propagation delay. The propagation delay has a shorter duration than the access time. The delay is assumed to have a uniform distribution over $[\pi, -\pi]$.

At the RAP, the signal has already experienced fading, path loss and additive noise in the air interface. This signal goes through a bandpass filter that suppresses out of band noise and separates it into corresponding systems. Then, separate amplifiers boost the separated signals to compensate attenuation in air. Finally, the signal directly modulates the laser.

The quality of the signals is indicated by the SNR. The following information is used to evaluate the ratios: i) the received power of WLAN signal is $P_{o,i}$, ii) each amplifier is assumed to have a noise figure of $F$, and iii) the bandpass filter has bandwidth of $B_{wlan}$ for WLAN signal.

The SNR for the WLAN signal can be written as follows:

$$\text{SNR}_{up} = \frac{P_o}{N_{up,wl}\, B_{wlan}\, F}. \tag{4.17}$$

The WLAN system does not have interference because only one user is transmitting for all successful transmission.

The actual signal that modulates the laser expressed in the time domain can be written as follows:

$$s_{laser}(t) = \sqrt{G_{up}}\left[s_{wlan}(t - \tau_\beta) + n_{up}(t)\right] \tag{4.18}$$

Both signal and noise are amplified by the power amplifiers with gain of $G_{up}$. Then, the bandpass filters at the RAP filter out of band noise. Assuming bandpass filters are ideal, the PSD of the noise signal $n_{up}(t)$ can be expressed as follows:

$$\Phi_{up}(\omega) = \frac{N_{up}\, F}{2}\left[rect\left(\frac{\omega - \omega_\beta}{\omega_{wlan}}\right) + rect\left(\frac{\omega + \omega_\beta}{\omega_{wlan}}\right)\right]. \tag{4.19}$$

Also, the RF power of the noise can be expressed as follows:

$$\langle n_{up}^2 \rangle = N_{up}\, F\, B_{wlan}. \tag{4.20}$$

In the RoF link, the RF power of a modulated signal is indicated by its optical modulation index. The power is proportional to the square of the optical modulation index. The optical modulation index of a WLAN signal, $m_{wlan}$, is defined as $B_\beta \sqrt{G_{up}}$. The optical modulation index is also Rayleigh distributed. The reasons are: first $B_\beta$ is Rayleigh distributed, second the power amplifier has fixed gain $G_{up}$. Another optical modulation index, which is known as the cumulative RMS optical modulation index, is defined as the square root of the total RF power that modulates the laser. The cumulative RMS optical modulation index $\mu$ is given as:

$$\mu = \sqrt{G_{up,wlan}} \left( \frac{B_\beta^2}{2} \right) = \sqrt{\frac{m_{wlan}^2}{2}}. \tag{4.21}$$

This RMS optical modulation index is a random process that is dependent on the square of the Rayleigh distributed random variable $m_{wlan}$ that expressed in the latter part of the expression (4.21).

Using the defined optical modulation index, the signal (4.18) that modulates the laser can be rewritten as follows:

$$s_{laser}(t) = m_{wlan}\, \frac{1}{N} \sum_{k=0}^{N-1} B_\beta\, a_{k,i}(t - \tau_\beta)\, expj2\pi k \frac{(n - N_g)}{N}\, \cos(\omega_\beta t - \phi_\beta) + n_{up,air}(t), \tag{4.22}$$

$$n_{up,air}(t) = \sqrt{G_{up}}\, n_{up}(t). \tag{4.23}$$

Knowing the optical modulation index, we can determine the required RF power gain for signals received at the RAP. The gain is first calculated with a pre-selected optical modulation index that has been optimized for performance in the RoF link, it can then be worked out from the two expressions that are as followed. For the WLAN system the gain is expressed as:

$$G_{up} = \frac{\overline{m_{wlan}^2}}{\overline{B_\beta^2}} \tag{4.24}$$

where, $\overline{B_\beta}$ are the average values for signal amplitude.

Graded index multimode fibre plays an important role here and propagates optical signal from photo diode. The impulse response of $\alpha$ profile multi-mode fibre can be expressed:

$$h_{MMF}(t) = \begin{cases} \frac{\alpha+2}{\alpha} |\frac{\alpha+2}{\Delta(\alpha-2)}|^{(2/\alpha)+1} |t|^{2/\alpha} \ except \ for \ \alpha \neq 2 \\ \\ \frac{2}{\Delta^2} \qquad\qquad\qquad\qquad\qquad for \ \alpha \approx 2 \end{cases} \tag{4.25}$$

The quality impairment in the RoF link is due to optical noise. The time domain noise term in the RoF link is written as $n_{opt}(t)$ and it is assumed to be an additive white Gaussian noise process. The noise is categorized into shot noise, thermal noise, and relative intensity noise [57].

The relative intensity noise originates from the laser and it is depended on both the square of the photocurrent and the cumulative RMS optical modulation index $\mu$ [57].

However, the shot noise and the thermal noise are independent of the modulation index $\mu$.

The general power expression is given as follows:

$$\langle n_{opt}^2 \rangle = RIN \, I_p^2 \, B \, (1 + \mu^2) + 2qI_pB + \frac{4 \, k_B \, T_o}{R_L} \tag{4.26}$$

The RoF link noise power for the WLAN system is $\langle n_{opt}^2 \rangle$ when $B = B_{wlan}$.

Applying the model, the photocurrent is expressed as follows:

$$i_D(t) = \frac{1}{\sqrt{F_{loss,dB}}} \left[ s_{laser}(t) * h_{MMF}(t) \right] + n_{opt}(t) \tag{4.27}$$

$$\approx \frac{1}{\sqrt{F_{loss,dB}}} \left[ s_{laser}(t) * h_{MMF}(t) - n_{up,air}(t) \right] + n_{opt}(t) \tag{4.28}$$

where, $F_{loss,dB}$ is the total RF power loss in the RoF link that is defined in expression 4.7, $s_{laser}$ is the input signal to the laser that is defined in (4.22), and $n_{opt}(t)$ is the noise in the link. The total RF power loss in the RoF link is dependent on the distance of its link. The

DC component of the photocurrent is omitted because it will be removed by the bandpass filter. The noise induced from the air interface is part of the signal, $s_{laser}$, that modulated the laser.

The cumulative OSNR of a WLAN signal is given as:

$$OSNR_{up} = \frac{m^2 \, I_D^2 \, E[s^2(t)] \, F_{loss,dB}}{(G_{up}) \, \langle n_{up}^2 \rangle + \langle n_{opt}^2 \rangle}. \qquad (4.29)$$

where, the noise power from air $\langle n_{up}^2 \rangle$ are given in (4.20), and $\langle n_{opt}^2 \rangle$ is the optical noise power for the WLAN system when $B = B_{wlan}$ in (4.26).

## 4.4   The Bit Error Rate

The basic statistical model in optical communication is the Poisson process because of the discrete photons. Despite this, the Gaussian density is often used to obtain probability of error expressions. Furthermore, when noise depends on the RF signal, which is Gaussian distributed, the optical noise is also Gaussian. Therefore, $\eta$ is modeled as a zero mean Gaussian process.

The component $\zeta$ in the expression for $Z_1$ represents the contribution of MAI in the decision statistic. $\zeta$ is the summation of $K - 1$ terms of $I_k$.

$$\zeta = \sum_{k=2}^{K} I_k \qquad (4.30)$$

According to the central limit theorem, $\zeta$ is a zero mean Gaussian random variable as $K - 1$ gets large. Therefore, the variance of $\zeta$ is given by,

$$\sigma_\varsigma^2 = \frac{N \, T^2}{6} \sum_{k=2}^{K} P_k \qquad (4.31)$$

where, $N$ is the length of the code and $T$ is the time. Now, the decision statistic $Z_1$ is modeled as a Gaussian random variable with mean $I_0$ and variance $\sigma_\varsigma^2 + \sigma_\eta^2$,

$$\sigma_\varsigma^2 + \sigma_\eta^2 = \frac{N \, T^2}{6} \sum_{k=2}^{K} P_k + \frac{N_0 T_b}{4} \qquad (4.32)$$

Because of the Gaussian assumption, the average bit error rate (BER) probability is given by:

$$BER = Q\left(\frac{\sqrt{\frac{P_0}{2}}T_b}{\sqrt{\frac{N\,T^2}{6}\sum\limits_{k=2}^{K}P_k + \frac{N_0 T_b}{4}}}\right) \tag{4.33}$$

$$BER = Q\left(1\left/\sqrt{\frac{1}{3N}\sum\limits_{k=2}^{K}\frac{P_k}{P_0} + \frac{N_0}{2T_b P_0}}\right.\right) \tag{4.34}$$

Assuming perfect power control, where, $P_k = P_o \ \forall \ k = 1, 2, 3, ....K$, the BER is,

$$BER = Q\left(\sqrt{\frac{3N}{K-1} + \frac{N_0}{2T_b P_0}}\right) \tag{4.35}$$

In this expression, the BER is evaluated assuming the average value for the variance of MAI. Typically, the above Gaussian approximation is very close to the values obtained by simulation when the number of users are above 15. When it is less than 15, then the BER is little more pessimistic.

## 4.5   Summary

In this chapter, a detailed analysis of COFDM-RoF are described and feasibility of using Graded index multi-mode fibre for indoor communication system was investigated. We used optimized equation of impulse response of Graded index fibre and considered all optical noises, splicings, and connectors losses for estimating optical signal to noise ratio and cumulative signal to noise ratio in RoF link. Also, we investigated the BER performance of a coded orthogonal frequency division multiplexing (COFDM) scheme that deploy the ROF link to provide wireless access to multiple users.

# Chapter 5

# Numerical Results and Discussions

This section describes the numerical results generated to evaluate the cumulative SNR, OSNR, and BER using various system parameters. The parameters and constant used in the simulation are listed in Table 5.1, and Table 5.2. These parameters are obtained from the values typically specified in the manufacturer's data sheets, technical specifications, or experimental values in previous publications. Note that the simulation is intended to get the tentative behavior. Nevertheless, the overall trend of the relative performance will remain the same and our objective is to study only the relative performance.

## 5.1 Downlink Results

In the downlink, the signal first goes through the RoF link then the air interface. The cumulative SNR is evaluated at the mobile station. The ratio includes the cumulative impairments from the air interface and the RoF link and the nonlinear distortion from the RoF link. Figures 5.1 to 5.6 are the results generated for the downlink. The OSNR of a WLAN

| OFDM symbol duration | $102.4\mu$ sec |
| --- | --- |
| FFT size | 256 |
| Number of subcarrier | 200 |
| Cyclic prefix | 64 |
| Cyclic prefix duration | 800 nsec |
| Modulation | BPSK |

**Table 5.1:** Wireless system parameters for the numerical results

| $G_{wlan}$ | RF power gain for WLAN signal | 20 dB |
|:---:|:---|:---:|
| $F$ | RAP/Receiver amplifier noise factor | 1 dB |
| $B$ | Bandwidth of signal | 22 MHz |
| $P_o$ | Laser mean optical power | 1 mW |
| $G_m$ | Laser modulation gain | 0.12 W/A |
| $\Re$ | Photo diode responsivity | 0.75 A/W |
| $n_c$ | Number of optical connectors | 2 |
| $l_c$ | Optical connector loss | 1 dB |
| RIN | Relative intensity noise parameter | $-155$ dB/Hz |
| $T_o$ | Optical receiver temperature | 275 K |
| $R_L$ | Receiver load resistance | 50 $\Omega$ |
| $\Delta$ | Refractive index difference | 0.02 |
| $\alpha$ | Core refractive index parameter | 4 |

**Table 5.2:** Optical system parameters for the numerical results

signal is referred to expression (4.9). The major system parameters used in the plots are: the cumulative RMS optical modulation index $\mu$, the length of the radio over fiber link, the distance between a MS and the RAP, and the distance between a WLAN MS and the RAP. The rest of the parameters and constants are listed in the table 5.2.
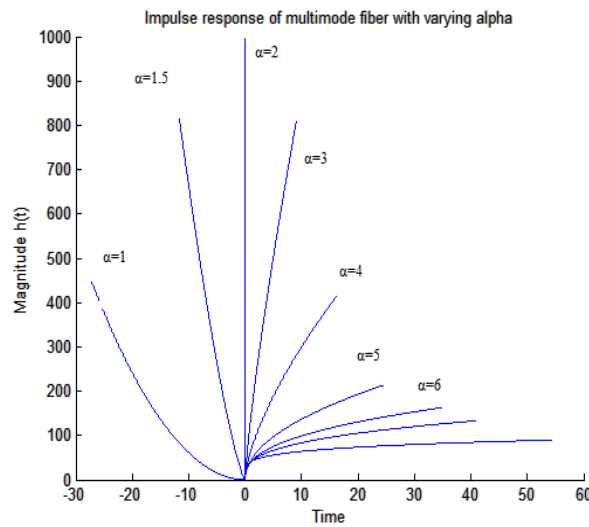


**Figure 5.1:** Impulse response of multi-mode fibre with $\alpha$ profile

Figure 5.1 shows the effect of change in the $\alpha$ to the impulse response of the channel for 10 km of multimode fibers can be seen. Although there is a very high performance improvement

when the optimum profile is achieved, a slight shift from the optimum profile may result in critical performance loss. It should also be noted that as $\alpha$ goes to $\infty$, the impulse spread $T$ is largest and the waveform of the impulse is flat-tapped and the fibre becomes a classical step index fibre.

As the $\alpha$ decreases, the impulse response becomes narrower, until at $\alpha = 2$, where it becomes the narrowest. When $\alpha < 2$, higher order modes arrive earlier than the lowest mode $(X = 0)$. This value suggests that the multi-mode dispersion could be reduced by shaping the core refractive index profile properly.
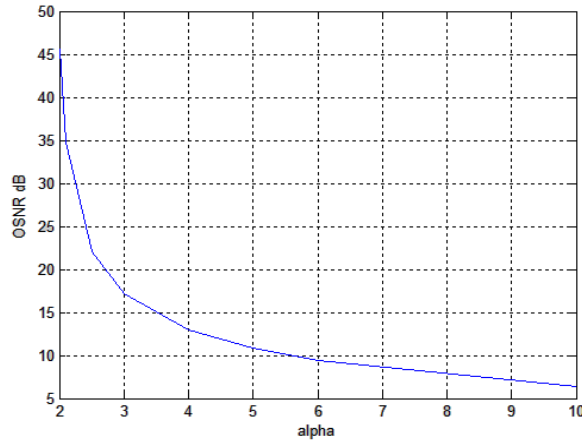


**Figure 5.2:** OSNR versus $\alpha$ profile

In Figure 5.2, it is observable that the OSNR decreases as $\alpha$ increases, resulting from either an increase in the fibre length or an increase of the $\alpha$ parameter of the fibre, are compensated by the cyclic prefix up until some point. When $\alpha$ reaches its optimal value we get the maximum OSNR.

Figure 5.3 illustrates the relationship between the system performance in terms of the cumulative SNR and the distance between a mobile station and the radio access point. A downward trend in the performance versus the distance is observed. This means that the optical noise is dominant but also the nonlinear distortion played an important role in RoF link. However, when the RoF is operated at the optimal value, the cumulative SNR is better
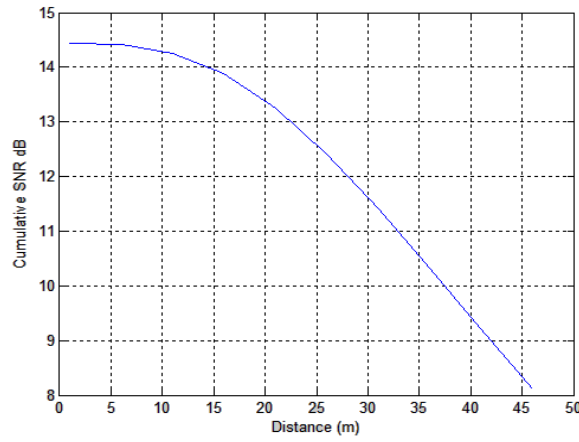
**Figure 5.3:** Cumulative SNR versus distance

than the rest even for a 10 km RoF link.
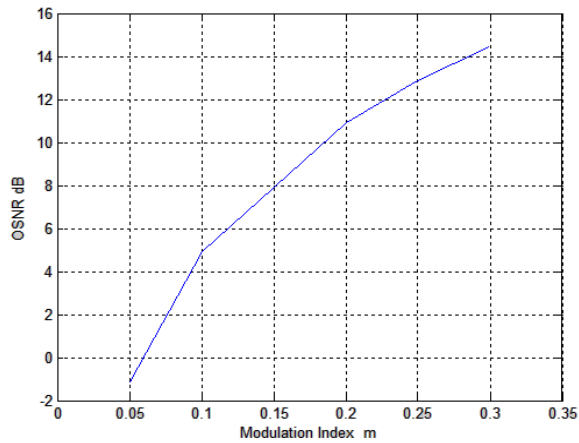


**Figure 5.4:** OSNR versus Optical modulation index

As depicted in Figure 5.4, and observed from the Eqn.(5.9) that the OSNR is the function of optical modulation index. The optical modulation index must be selected to avoid the over-modulation. Figure 5.4 illustrates that at low modulation index, optical device noise is dominant and the OSNR increases with modulation index up to 0.3. At high modulation index, the nonlinear effect becomes larger and OSNR increases slowly with modulation index.

Within the range from 0.05 to 0.3, the maximal OSNR is more than 15 dB.
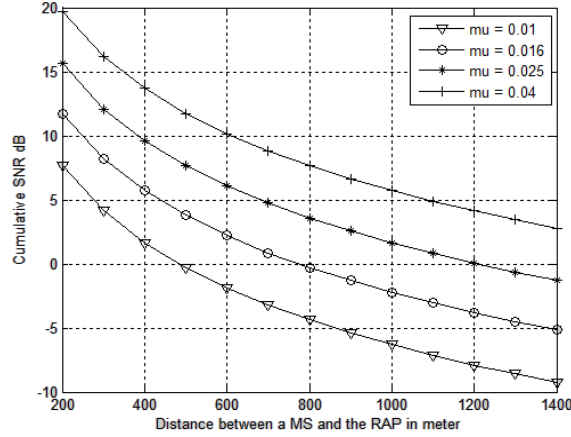


**Figure 5.5:** Distance between a MS and the RAP

Figure 5.5 illustrates the relationship between the system performance and the distance between a MS and the RAP in a different way. Figure shows the different curves with various lengths of RoF link with an optimal $\mu$ used. It is very interesting to see that for small index $\mu$, the cumulative SNR improves inversely with the distance. While at large index value, the performance is almost independent of distance between mobile station and the radio access point. The reason is that the nonlinear distortion is much larger than the noise in the air interface.

Figure 5.6 illustrates the same trend as Figure 5.5 but different index $\mu$. When $\mu$ is small, the performance deteriorates with the distance. When $\mu$ is large, the performance is independent of the distance.

Figure 5.7 shows the BER performance for coded orthogonal frequency division multiplexing radio-over-fibre communication system. Figure illustrates how the BER varies with SNR values, where the transmission channel is added with optical noises, and air impairments. Here the BER values are reduced with increment of SNR values.
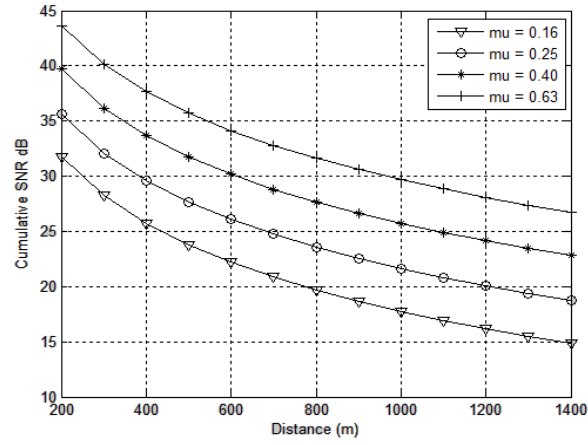
**Figure 5.6:** Distance between a MS and the RAP
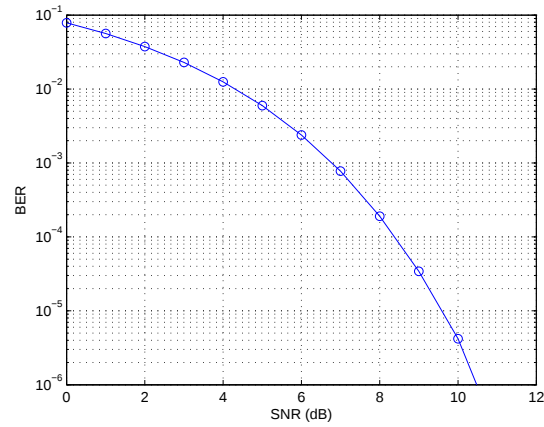


**Figure 5.7:** BER performance for COFDM-RoF system

## 5.2   Uplink Results

For the uplink, the numerical results generated are the SNR and OSNR ratios versus various system parameters. Figures 5.7, 5.8 and 5.9 are the results generated for the uplink. In the uplink, the signal first goes through the air interface then the RoF link. The cumulative OSNR is evaluated at the end of the RoF link where the central base station is. The ratios include cumulative impairments from the air interface and the RoF link including the additive noise in both interfaces and the nonlinear distortion from the RoF link. We assumed that signal is experienced the same noise spectrum in the air interface.

The cumulative OSNR of a WLAN signal is referred to expression (4.29). The major system parameters used in the plots are: the cumulative RMS optical modulation index $\mu$ (4.21), the length of the RoF link, and the SNR for a WLAN signal at the RAP $SNR_{up}$. The rest of the parameters and constants are listed in the table 5.2. Notice that the cumulative RMS optical modulation index $\mu$ has the same expression for both uplink and downlink, but each expression has slight difference in meaning and, thus, should not treat them as they are equal.

In Figure 5.7, the OSNR of a WLAN signal versus the index $\mu$ is plotted. The nonlinear distortion comes into effect for large $\mu$, and the optical noise comes into effect for very small $\mu$. Actually, for small $\mu$ the effect of optical noise can be observed from this plot where longer RoF link has lower OSNR ratio. However, for the useful range of the index $\mu$ (0.01-0.6) the OSNR does not change with the length of the ROF link.

A conclusion can be drawn that in the useful range of $\mu$ the quality of the signal is not affected by the length of the RoF link. In addition, the cumulative OSNR ratios remain very much constant for the useful range. That means smaller power (smaller $\mu$) can achieve the similar performance. We know that the square of the cumulative RMS optical modulation index is equivalent to the total RF power that modulates the laser.

The cumulative OSNR of a WLAN signal versus the $SNR_{up}$ is plotted in Figure 5.8. The $SNR_{up}$ is the SNR for a WLAN signal at the RAP. It is used as a reference for the signal quality that enters the RoF link. The signal quality concerns here is the noise spectrum of
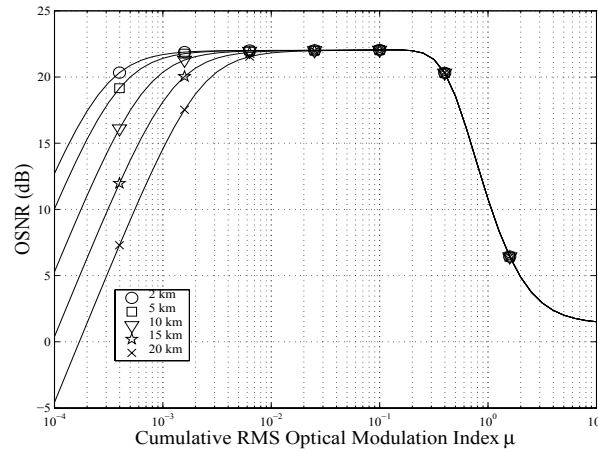
**Figure 5.8:** OSNR vs Cumulative RMS optical modulation index $\mu$

the air interface, so the $SNR_{up}$ is really to reflect the amount of noise from the air interface. Also, the WLAN system has a stronger dependency on the SNR at the RAP. In the figure, it can be observed that the cumulative OSNR improved far beyond 20 dB of SNR at the RAP. It shows that in the range of SNR from 1 dB to 45 dB the cumulative OSNR increases with the SNR. It is seemed that the quality of the systems is independent of the length of the RoF. However, the independency is true for the value of $\mu$ when $\mu$ is 0.5.
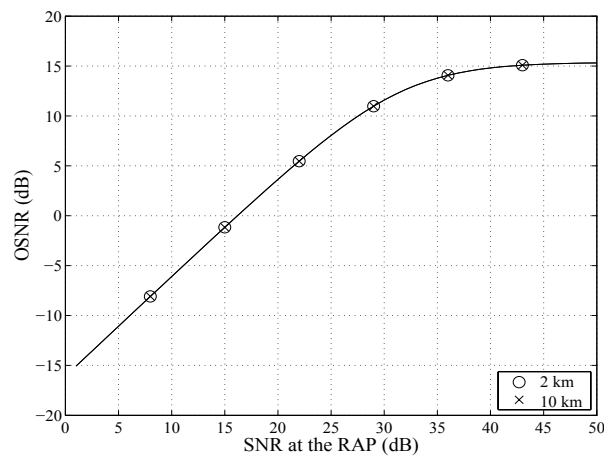


**Figure 5.9:** The OSNR vs the SNR at the RAP

Figure 5.9 shows the three curves generated for the three different values of $\mu$. In this figure, the trend of dependency on the SNR at the RAP is observed. The WLAN system has stronger dependency on the SNR. Furthermore, the SNR reduces as the cumulative optical modulation index $\mu$ increases. This figure shows that the OSNR does not improve when SNR is larger 20 dB for small $\mu$, and then for a larger $\mu$ the OSNR saturates beyond 10 dB of SNR. This can be explained that larger $\mu$ causes more nonlinear distortion in the RoF that limits the overall performance of the system.
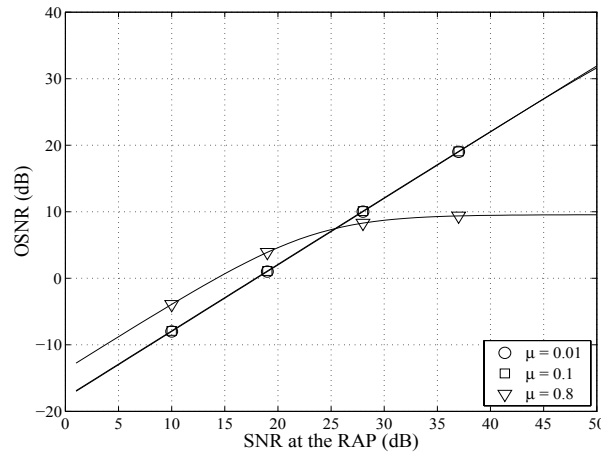


**Figure 5.10:** The OSNR of a WLAN signal vs the SNR at the RAP

Figure 5.11 shows the BER curves in the noise limited region. The effect of combined noise is seen in the BER performance with two or three users. As the number of users increases, the BER curve flattens because, with filter detectors, a COFDM system when the interference power exceeds the noise power. Here, the overall BER performance is very good because of large $N$, coded OFDM, and few users.

Figure 5.12 shows the bit error probability curve for COFDM-RoF system. We can observe form the curve that the BER is very reasonable for SNR because of coded OFDM signal and a low dispersive MMF. The result show that using COFDM with MMF allows the BER to be improved in a noisy channel. Using BPSK the COFDM transmission can tolerate a SNR of $> 8 - 10$ dB.
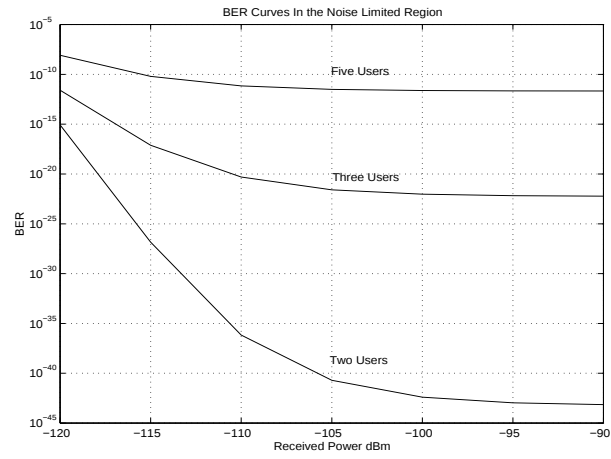
**Figure 5.11:** BER curves of RoF system in the noise limited region
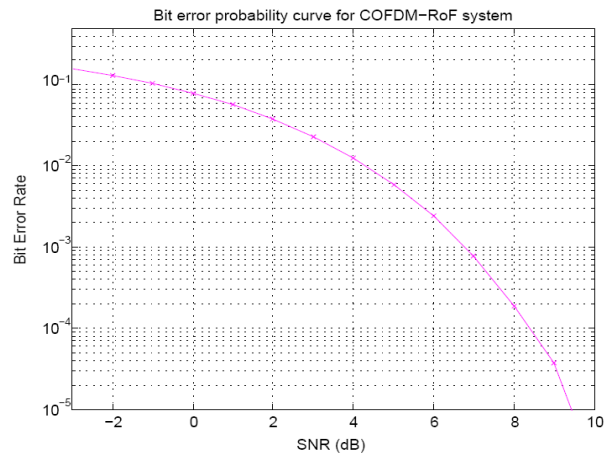


**Figure 5.12:** Bit error probability curve for COFDM-RoF system

## 5.3 Summary

This chapter presented and explained the numerical results of proposed architecture. We evaluated the approximate equations for the purpose of justifying the proposed derivation method. This chapter divided into two parts: In the first part we presented downlink results and second part described uplink results. In the downlink, the signal first goes through the Fiber-Wireless link then the air interface. The system performance is limited by the nonlinear distortion of Fibre-Wireless link when the cumulative RMS optical modulation index is large. The results have shown that the length of the Fibre-Wireless link does matter. The optical noise was the dominant source of impairments in this case. In the uplink, the system should operate $\mu$ in the range of 0.01 to 0.1. In this range of $\mu$, the system performance was not dependent on the fiber length. As shown in our simulations, as long as the fiber length is reasonable, graded index multi-mode fibres, even step index multi-mode fibres can be used for Fibre-Wireless systems.

# Chapter 6

# Conclusions and Future Work

In this thesis, the COFDM-RoF architecture is investigated and then the fibre based radio access mechanisms for the air interface and the RoF link are evaluated. In the air interface, the signals experience path loss and multipath fading. These impairments are linear. In the RoF link, the signals experience both linear and nonlinear impairments. The linear impairments are the RIN, shot noise, thermal noise, and the power loss. Finally, the downlink and uplink analysis that accounts for the cumulative effects for all the impairment is carried out.

In the numerical results, the performance of both proposed systems are evaluated in terms of cumulative SNR, OSNR, and BER using various system parameters. In the downlink, the signal first goes through the RoF link then the air interface. The cumulative SNR is evaluated at the mobile station. The ratio includes the cumulative impairments from the air interface and the RoF link and the nonlinear distortion from the RoF link. The system performance is limited by the nonlinear distortion of RoF link when the cumulative RMS optical modulation index is large. Large $\mu$ means large RF power modulates the laser. When $\mu$ is larger than the optimal range, excessive nonlinear distortion deteriorates the system performance. The results have shown that the length of the RoF link does matter. The optical noise is the dominant source of impairments in this case. In the uplink, the system should operate $\mu$ in the range of 0.01 to 0.1. In this range of $\mu$, the system performance is not dependent on the fiber length.

As shown in our simulations, as long as the fibre length is reasonable, graded index multi-mode fibres, even step index multi-mode fibres can be used for RoF systems. For those systems, the dispersion is compensated by the CP.

The combined performance evaluation and investigation of the imperfections jointly for wireless and fibre systems appear as a promising area of research. Although the work presented in this thesis is a first step in that direction, it already achieved some important conclusions. I believe the collaborative view of optical and wireless systems will continue to help solving problems which is harder to solve when the two systems are isolated from each other.

## 6.1 Research Contributions

The major contributions we achieved are:

- Investigates the downlink and uplink in terms of optical signal to noise, and cumulative signal to noise ratios considering both optical and wireless channel impairments,

- The finding of this thesis will be helpful for the system designers to determine the RF power and to predict cell sizes, OSNR, SNR, and BER performances of the system,

- The low installation and maintenance costs associated with using Graded index multi-mode fibre,

- The limitation in multi-mode fibre bandwidth caused by dispersion is overcome by employing cyclic prefix,

- Optimized impulse response of Graded index fibre and can be used for reasonable fibre length.

### 6.1.1 Major Observations

The detailed analysis reveals some interesting information. The major observations are:

- Within the linear, optical noise limited region, increasing the cumulative modulation index $\mu$ improves the performance of the system. However, too large $\mu$ drives both system into nonlinear region severely affecting performance,

- There is an inverse relationship between the fiber length and the radio cell size. This is due to cumulating losses, distortion and noise in both optical and wireless channels,

- The optical and wireless SNRs depend on the fibre length, optical to electrical and electrical to optical conversion losses, radio cell sizes and the relative RF power of both systems.

We evaluated the approximate equations for the purpose of justifying the proposed derivation method. The parameters used for the link performance are obtained from the values typically specified in the manufacturer's data sheets, technical specifications, or experimental values in previous publications. Note that the simulation is intended to get the tentative behaviour; we do not strictly rely on the simulation parameters which may vary. Nevertheless, the overall trend of the relative performance will remain the same and our objective is to study only the relative performance.

Overall, our analysis helps to find better system parameters for the system and interrelationship between the fibre length, the radio cell size and the signal to noise ratio. Nevertheless, better design and low noise, and linearized fiber optic transceivers will improve the performance.

## 6.2   Future Works

For possible future work, alternative architectures in both directions (uplink & downlink) that simultaneously support 4G network standards should be investigated. A possible architecture is to transmit WLAN signal over fibre systems operating at 60 GHz. The architecture can use mostly off the shelf components and cost saving is possible. The WLAN signals are in the baseband digital format from the core network, which will make it easy to transmit.

The effectiveness of such architecture requires similar analysis that is done in this thesis. Also, for the same architectures one may use Polymer optical fiber (POF) and evaluate the performance for indoor environment.

# Bibliography

[1] Arun N. Netravali, "Networking Becomes Second Nature: The Next 25 Years and Beyond," *Bell Labs Technical Journal*, no. 5, pp. 203 - 214, 2000.

[2] S. Ohmori and Y.Yamao and N. Nakajima, "The Future Generations of Mobile Communications based on Broadband Access Technologies," *IEEE Communications Magazine*, vol. 38, no. 12, pp. 134 - 142, 2000.

[3] S. Kanprachar and I. Jacobs, "Bandpass Transmission Characteristics of Multimode Fiber," *presented at Optics in the Southeast Meeting 2001, Clemson University, South Carolina*, 2001.

[4] Bryn J. Dixon and Roger D. Pollard and Stavros Iezekiel, "Othogonal Frequency-Division Multiplexing in Wireless Communication Systems With Multimode Fibre Feeds," *IEEE Transactions on Microwave Theory and Techniques*, vol. 49, no. 8, pp. 1404 - 1409, 2001.

[5] X. N. Fernando and A. Anpalagan, "On the design of optical fiber based wireless access systems," *Proceedings of International Conference on Communication*, pp. 3550 - 3555, 2004.

[6] A.M. Matarneh and S.S.A Obayya, and I.D. Robertson, "Coded Orthogonal Frequency Division Multiplexing (COFDM) Transmission over Graded-Index Multimode Fibre," *IEEE Conference on PhotonicsGlobal*, pp. 1-4, IPGC 2008.

[7] S.C. J. Lee and F. Breyer and S. Randel and H.P.A. van den Boom and A.M.J. Koo-

nen, "Orthogonal Frequency Division Multiplexing over Multimode Optical Fibers," *Proceedings Symposium IEEE/LEOS Benelux Chapter, Brussels*, 2007.

[8] A. Pizzinat and P. Urvoas and B. Charbonnier, "1.92G bit/s MB-OFDM Ultra Wide Band Radio Transmission over Low Bandwidth Multimode Fibre," *Optical Fibre Communication and the National Fibre Optic Engineers Conference*, pp.1-3, 2007.

[9] F. Tabatabai and H. Al-Raweshidy, "Performance Evaluation for WLAN and UWB Using Radio over Fibre," *The 9th European Conference on Wireless Technology*, pp.147-149, 2006.

[10] J. Armstrong, "OFDM for optical communications," *Journal of lightwave technology*, vol. 27, no. 3, pp. 189 - 204, 2009.

[11] A. Das and A. Nkansah and N.J. Gomes and I.J. Garcia and J.C. Batchelor and D. Wake, "Design of low-cost multimode fibre-fed indoor wireless networks," *IEEE Transactions on Microwave Theory and Techniques*, vol.54, no.8, pp.3426-3432, 2006.

[12] N.J. Gomes and A. Das and A. Nkansah and I.J. Garcia and J.C. Batchelor and D. Wake, "Multimode Fibre-fed Indoor Wireless Networks," *IEEE International Topical Meeting on Microwave Photonics*, pp.1-4, 2006.

[13] C. Carlsson and A. Larsson and A. Alping, "RF transmission over multimode fibres using VCSELs-comparing standard and high-bandwidth multimode fibres," *Journal of Lightwave Technology*, vol. 22, no.7, pp. 1694- 1700, 2004.

[14] X. N. Fernando, "An improved expression for dynamic relative intensity noise in radio over fiber applications," *IEEE Transactions on Communications*, 2004.

[15] H. Kim and Y. C. Chung, "Passive optical network for CDMA-based microcellular communication systems," *Journal of Lightwave Technology*, pp. 301 - 311, 2001.

[16] J. C. Fan and C. L. Lu and L. G. Kazovsky, "Dynamic Range Requirements for Microcellular personal communication systems using analog fiber-optic links," *IEEE Transations on Microwave Theory and Techniques*, no. 8, pp. 1390 - 1397, 1997.

[17] Marwanto, and Arief, and M. Idrus, and Sevia and A. Suryani, "The SCM/WDM System Model for radio over Fiber Communication Link," *IEEE International RF and Microwave Conference*, pp. 400 - 403, 2008.

[18] S.S.H. Yam and F. Achten, "Single wavelength 40 Gbit/s transmission over 3.4 km broad wavelength window multimode fibre," *Electron Letter*, vol. 42, no. 10, 2006.

[19] S.C.J. Lee, and F. Breyer, et al., "24-Gb/s Transmission over 730 m of Multimode Fiber by Direct Modulation of an 850-nm VCSEL using Discrete Multi-tone Modulation," *National Fiber Optic Engineers Conference, OSA Technical Digest Series (CD), Optical Society of America*, PDP6, 2007.

[20] N.E. Jolly, et al., "Generation and propagation of a 1550nm 10 Gbit/s Optical Orthogonal Frequency Division Multiplexed signal over 1000m of Multimode fibre using a directly modulated DFB ," *Proc OFC'05*, OFP3, 2005.

[21] J.M. Tang and K.A. Shore, "Maximizing the Transmission Performance of Adaptively Modulated Optical OFDM Signals in Multimode-Fiber Links by Optimizing Analog-to-Digital Converters," *Journal of lightwave technology*, vol. 25, no. 3, pp. 787-798, 2007.

[22] Tutorial on, "COFDM," *Digital Radio Technology. May 2008. Available online at http://www.digitalradiotech.co.uk/cofdm.htm*, last accessed on January 3rd, 2010.

[23] William Shieh and Ivan Djordjevic, "OFDM for Optical Communications," *Elsevier Academic Press, San Diego, CA, USA*, Edition 1st, 2010.

[24] John M. Senior, "Optical Fiber Communications: Principles and Practice," *Prentice Hall*, Edition 3rd, 2009.

[25] John A. C. Bingham, "Multicarrier Modulation for Data Transmission: An Idea Whose Time Has Come," *IEEE Communications Magazine*, vol. 28, pp. 5 - 14, May 1990.

[26] William Y. Zou and Yiyan Wu, "COFDM: An Overview," *IEEE Transactions on Broadcasting*, vol. 41, no. 1, pp. 1 - 8, March 1995.

[27] William Y. Zou and Yiyan Wu, "Orthogonal Frequency Division multiplexing: A Multi-Carrier Modulation Scheme," *IEEE Transactions on Consumer Electronics*, vol. 41, no. 3, pp. 392 - 399, August 1995.

[28] S. B. Weinstein and Paul M. Ebert, "Data Transmission by Frequency-division Multi-plexing Using the Discrete Fourier Transform," *IEEE Transactions on Communication Technology*, vol. COM-19, no. 5, pp. 628 - 634, October 1971.

[29] Botaro Hirosaki, "An Orthogonally Multiplexed QAM System Using the Discrete Fourier Transform," *IEEE Transactions on Communications*, vol. COM-29, no. 7, pp. 982 - 989, July 1981.

[30] Qun Shi, "Error Performance of OFDM-QAM in Subcarrier Multiplexed Fiber Optic Transmission," *IEEE Photonics Technology Letters*, vol. 9, no. 6, pp. 845 - 847, June 1997.

[31] Bryn J. Dixon and Roger D. Pollard and Stavros Iezekiel, "Orthogonal Frequency Division Multiplexing in Wireless Communication Systems with Multimode Fiber Feeds," *IEEE Transactions on Microwave Theory and Techniques*, vol. 49, no. 8, pp. 1404 - 1409, August 2001.

[32] Hideki Ochiai and Hideki Imai, "Block Codes for Frequency Diversity and Peak Power Reduction in Multicarrier Systems," *Information Theory*, pp. 192, August 1998.

[33] Mohammad G. Rahman and R. M. Rajatheva and Kazi M. Ahmed, "Performance of Serial Concatenated Convolutional Code in Rayleigh Multipath Fading Channel," *IEEE Vehicular Technology Conference*, vol. 5, no. 8, pp. 2510 - 2514, 1999.

[34] Klaus Witrisal and Yong-Ho Kim and Ramjee Prasad, "A Novel Approach for Performance Evaluation of OFDM with Error Correction Coding and Interleaving," *IEEE Vehicular Technology Conference*, pp. 294 - 299, 1999.

[35] J. F. Helard and B. Le Floch, "Trellis Coded Orthogonal Frequency Division Multiplexing for Digital Video Transmission," *IEEE Global Telecommunications Conference*, pp. 785 - 791, 1991.

[36] A. D. Jayalath and R. M. Rajatheva, " Coded Orthogonal Frequency Division Multiplexing for Wireless ATM," *IEEE Vehicular Technology Conference*, pp. 2049 - 2053, 1999.

[37] A. Doufexi and E. Tameh and A. Nix and S. Armour and A. Molina, "Hotspot wireless LANs to enhance the performance of 3G and beyond cellular networks," *IEEE Communications Magazine*, vol. 41, no. 7, pp. 58 - 65, July 2003.

[38] U. Varshney, "The status and future of 802.11-based WLANs," *IEEE Computer*, vol. 36, no. 6, pp. 102 - 105, June 2003.

[39] Muhammad Imadur Rahman and Suvra Sekhar Das and Frank H.P. Fitzek and Talwalkar Rohit, "OFDM Based WLAN Systems," *Center for TeleInFrastruktur (CTiF), Aalborg University, Denmark*, 2005.

[40] N. Dinur and D. Wulich, "Peak-to-average power ratio in high-order OFDM," *IEEE Transactions on Communications* , no. 6, pp. 1063 - 1072, 2001.

[41] I. Haroun, "WLANs Meet Fiber Optics Evaluting 802.11a WLANs Over Fiber Optic Links," *Available online at http://www.rfdesign.com*, last accessed on January 15th, 2010.

[42] O. K. Tonguz and H. Jung, "Personal Communications Access Networks Using Subcarrier multiplexed optical links," *Jounal of IEEE Lightwave Technology*, no. 6, pp. 1400 - 1409, 1996.

[43] S. D. Walker and M. Li and A. C. Boucouvalas and D. G. Cunningham and A. N. Coles, "Design techniques for subcarrier multiplexed broadcast optical networks," *IEEE Journal on Selected Areas in Communications*, pp. 1276 - 1284, 1990.

[44] R.R. Mosier and R.G. Clabaugh, "Kineplex, a bandwidth efficient binary transmission system," *AIEE Transactions*, pp. 723 - 728, 1958.

[45] Robert Chang, "Orthogonal Frequency Division Multiplexing," *US Patent 3488445, Field*, 1970.

[46] R. Chang, "Synthesis of Band-Limited Orthogonal Signals for Multichannel Data Transmission," *The Bell System Technical Journal*, pp. 1775 - 1796, 1996.

[47] S. B. Weinstein and Paul M. Ebert, "Data Transmission by Frequency Division Multiplexing using the Discrete Fourier Transform," *IEEE Transaction on Communication Technology*, no. 5, pp. 628 - 634, 1971.

[48] R. Prasad, "OFDM for wireless communications systems," *Artech House*, 2004.

[49] R. Van Nee and R. Prasad, "OFDM for wireless multimedia communications," *Artech House*, 2000.

[50] L. Litwin and M. Pugel, "The principle of OFDM," *Available online at http://voronuk.boom.ru/documents/ofdm.pdf*, last accessed on October 11th, 2010.

[51] Koffman. I and Roman. V, "Broadband wireless access solutions based on OFDM access in IEEE 802.16," *IEEE Communications Magazine*, no. 4, pp. 96 - 103, April 2002.

[52] W. C. Y. Lee, "Mobile communications Engineering," *New York: McGraw Hill*, Edition 2nd, 1997.

[53] T. K. Sarkar and Z. Ji and K. Kim and A. Medouri and M. Salazar-Palma, "A survey of various propagation models for mobile communication," *IEEE Antennas and Propagation Magazine*, no. 3, pp. 51 - 82, 2003.

[54] Sollenberger and N.R. Cimini and L.J., "Receiver structures for multiple access OFDM," *IEEE Vehicular Technology Conference* , pp. 468 - 472, 1999.

[55] T. K. Fong and M. Tabara and D. J. M. Sabido and L. G. Kazovsky, "Dynamic range of externally modulated analog optical links: optical amplification versus coherent detection," *IEEE Photonics Technology Letters*, pp. 270 - 272, 1994.

[56] P. Papazian, "Basic transmission loss and delay spread measurements for frequencies between 430 and 5750 MHz," *IEEE Transactions on Antennas and Propagation*, no. 2, pp. 694 - 701, 2005.

[57] J.Hecht, "Understanding Fiber Optics," *Prentice Hall*, Edition 2nd, 2002.

[58] Stavros Kotsopoulos and Konstantinos Loannou, "Handbook of Research on Heterousgeneous Next Generation Networking: Innovations and Platforms," *IGI Global*, Edition 1st, 2008.

[59] Takanori Okoshi, "Optical Fibers," *Academic Press, San Diego, CA, USA*, Edition 2nd, 1982.

[60] D. Gloge and E. A. J. Marcatili, "Multimode theory of graded-core fibers," *Journal of Bell Systems Technology*, pp. 1563 - 1578, November 1973.

[61] Gerd Keiser, "Optical Fiber Communications," *Boston, MA : McGraw-Hill*, Edition 5th, 2000.

[62] W. I. Way, "Subcarrier multiplexed lightwave system design considerations for subscriber loop applications," *Journal of Lightwave Technology*, no. 11, pp. 1806 - 1818, November 1989.

[63] Microwave Fiber Optics Group, "A System Designer's Guide to RF and Microwave Fiber Optics," *Ortel Corporation*, 1999.

[64] J. H. Stott, "The how and why of COFDM," *BBC Research and Development Tutorial,
1998. Available online at http://www.ebu.ch/en/technical/trev/trev_278-stott.pdf,* last
accessed on January 3rd, 2010.

[65] WiMAX Forum, "White paper on Mobile WiMAX  Part 1:  A Techni-
cal Overview and Performance Evaluation," *August 2006. Available online at
http://www.wimaxforum.org/technology/downloads/
Mobile_WiMAX_Part1_Overview_and_Performance.pdf,* last accessed on January 3rd,
2010.